

Fundamental computational limits of weak learnability in high-dimensional multi-index models

Emanuele Troiani¹, Yatin Dandi^{1,2}, Leonardo Defilippis³,
 Lenka Zdeborová¹, Bruno Loureiro³, and Florent Krzakala²

¹*Statistical Physics Of Computation Laboratory, École Polytechnique Fédérale de Lausanne (EPFL)*

²*Information Learning and Physics Laboratory, École Polytechnique Fédérale de Lausanne (EPFL)*

³*Departement d’Informatique, École Normale Supérieure, PSL & CNRS*

April 3, 2025

Abstract

Multi-index models — functions which only depend on the covariates through a non-linear transformation of their projection on a subspace — are a useful benchmark for investigating feature learning with neural nets. This paper examines the theoretical boundaries of efficient learnability in this hypothesis class, focusing on the minimum sample complexity required for weakly recovering their low-dimensional structure with first-order iterative algorithms, in the high-dimensional regime where the number of samples $n = \alpha d$ is proportional to the covariate dimension d . Our findings unfold in three parts: (i) we identify under which conditions a *trivial subspace* can be learned with a single step of a first-order algorithm for any $\alpha > 0$; (ii) if the trivial subspace is empty, we provide necessary and sufficient conditions for the existence of an *easy subspace* where directions that can be learned only above a certain sample complexity $\alpha > \alpha_c$, where α_c marks a computational phase transition. In a limited but interesting set of really hard directions —akin to the parity problem— α_c is found to diverge. Finally, (iii) we show that interactions between different directions can result in an intricate hierarchical learning phenomenon, where directions can be learned sequentially when coupled to easier ones. We discuss in detail the *grand staircase* picture associated to these functions (and contrast it with the original staircase one). Our theory builds on the optimality of approximate message-passing among first-order iterative methods, delineating the fundamental learnability limit across a broad spectrum of algorithms, including neural networks trained with gradient descent, which we discuss in this context.

1 Introduction

A fundamental property of neural networks is their ability to learn features and adapt to relevant structures in high-dimensional noisy data. However, our mathematical understanding of this mechanism remains limited. A popular model for studying this question is *multi-index models*. Multi-index functions are a class of statistical models encoding the inductive bias that the relevant directions for prediction depend only on a low-dimensional subspace of the covariates $\mathbf{x} \in \mathbb{R}^d$:

$$y = g(\mathbf{W}\mathbf{x}), \quad \mathbf{W} \in \mathbb{R}^{p \times d}, \quad (1)$$

where the mapping $g : \mathbb{R}^p \rightarrow \mathbb{R}$ can further be stochastic i.e. depend on independent noise $\xi \in \mathbb{R}^{p'}$ for some finite p' . They define a rich class of hypotheses (Li, 1991), containing many widely studied functions in the statistical learning and theoretical computer science literature. The simplest instance is the *Linear model* ($p=1$) given by a linear link function $g(z) = z$, or its noisy version $g(z, \xi) = z + \sqrt{\Delta}\xi$, with $\xi \sim \mathcal{N}(0, 1)$. In the *Single-index model* ($p=1$), also known as *generalised linear model*¹, $g(z)$ can be an arbitrary, possibly

¹More precisely, *single-index model* is employed in a context where both the direction \mathbf{w} and link function g are learned, while *generalised linear model* is used when the link function is known and only the weights are learned. In this work, we use both interchangeability.

stochastic, link function, including some widely studied problems such as *phase retrieval* $g(z) = z^2$ and the *perceptron* $g(z) = \text{sign}(z)$. Some example of multi-index models include the *Two-layer neural network* ($p > 1$), given by a link function $g(z_1, \dots, z_p) = \sum_{k=1}^p a_k \sigma(z_k)$; *Polynomial functions* ($p > 1$), given by any linear combination of products of z_1, \dots, z_p , for example $g(z_1, z_2, z_3) = 1 + z_1^2 z_2^2 - 2z_1 + z_2 z_3^3$; and *s-sparse parities* ($p > 1$) that can be embedded in a multi-index model by taking a link function $g(z_1, \dots, z_p) = \prod_{k \in I} \text{sign}(z_k)$ for any subset $I \subset [p]$ of size $|I| = s \leq p$. Training a multi-index model typically translates to a non-convex optimization problem. Several authors have thus used multi-index models as a test-bed for understanding the behavior of neural nets and gradient-descent in non-convex, high-dimensional contexts, e.g. (Saad and Solla, 1995; 1996; Arous et al., 2021; Abbe et al., 2022; 2023; Veiga et al., 2022; Ba et al., 2022; Arnaboldi et al., 2023; Collins-Woodfin et al., 2023; Damian et al., 2023; Bietti et al., 2023; Moniri et al., 2023; Berthier et al., 2023).

To serve as a useful benchmark, it is necessary to have an idea of the fundamental limit of learnability in such models. This translates to the question of how many observations from the model in Equation (1) are required to obtain a better-than-random prediction within a class of algorithms, also known as *weak learnability*. This can be studied both *statistically* (within the class of all, including exponential time algorithms) or *computationally* (restricted to a particular computational class, such as first-order algorithms). In the single-index case ($p=1$), weak learnability has been heavily studied under probabilistic assumptions for the weights and data distribution (e.g. i.i.d. Gaussian or uniformly in the sphere). The statistical threshold for learnability has been characterised by Barbier et al. (2019) when the covariate dimension d is large. Optimal computational thresholds for the class of first-order iterative algorithms were also derived in (Mondelli and Montanari, 2019; Luo et al., 2019; Celentano et al., 2020; Maillard et al., 2020). Algorithmic results were also proven for other computational models: Damian et al. (2022) provided a lower bound $n \geq d^{\max(1, \ell/2)}$ under the Correlational Statistical Query (CSQ) model, comprising algorithms that take queries of the type $\mathbb{E}[y\varphi(\mathbf{x})]$. Here ℓ denotes the *information exponent* (Arous et al., 2021) of the target defined as the first non-zero integer $\ell > 0$ in the Hermite expansion of g : $\ell = \min\{j \in \mathbb{N} : \langle g, \mathcal{H}_j \rangle_\gamma \neq 0\}$.

A related notion is that of staircase functions (Abbe et al., 2022; 2023), which characterizes the sample complexity for sequential learning of directions under the CSQ model or online SGD. For staircase functions, the CSQ sample complexity is governed by the “leap”, which informally equals the maximum jump in degree (in the Hermite expansion) conditioned on previously learned directions. For instance the target $g(z_1 z_2 z_3) = z_1 + z_1 z_2 + z_1 z_2 z_3$ has leap 1, since the term $z_1 z_2$ is linear conditioned on z_1 while $z_1 z_2 z_3$ is linear conditioned on z_1, z_2 . Additionally Damian et al. (2024) provided results for the Statistical Query (SQ) model, which allows for more flexible queries of the type $\mathbb{E}[\varphi(\mathbf{x}, y)]$, and a lower sample complexity $n \geq d^{\max(1, \kappa/2)}$ with $\kappa \leq \ell$ defining the *generative exponent*. As we shall see, our results allows to reconcile this picture with an *extended* version of staircase functions that we refer to as *grand staircase functions*.

Aside from the particular case of committee machines (Aubin et al., 2019; Diakonikolas et al., 2020; Goel et al., 2020; Chen et al., 2022), results for general multi-index models $p > 1$ are scarce, as they crucially depend on the way different directions are coupled by the link function. The goal of the present work is precisely to close this gap for the class of Gaussian multi-index models in the proportional, high-dimensional regime, and to provide a classification of how hard it is to learn feature directions from data in multi-index models. More precisely, our **main contributions** are:

- We analyse the computational limits of weak learnability (Def. 2) for Gaussian multi-index models in the class of first-order methods, in the high-dimensional limit when $d, n \rightarrow \infty$ at fixed ratio $\alpha = n/d$ and constant number of indices $p = \Theta(1)$. Our analysis leverages the optimality of Bayesian approximate message passing algorithms (AMP) (Donoho et al., 2009; Rangan, 2011) among first-order iterative methods (Zdeborová and Krzakala, 2016; Celentano et al., 2020; Montanari and Wu, 2022), allowing us to delineate the fundamental learnability limits across a wide range of algorithms, including neural nets trained with gradient descent.
- We provide a classification of which directions are computationally *trivial*, *easy* or *hard* to learn with AMP from linearly many samples: *trivial directions* can be learned with a single AMP iteration for any $\alpha > 0$. When no such direction exists, we show there might be *easy directions* allowing recovery from arbitrarily small side-information $\sqrt{\lambda} > 0$ in $\mathcal{O}(\log^{1/\lambda})$ steps with at least $n = \alpha_c d$ samples, where α_c marks a computational transition. Heuristically, we expect recovery along easy directions from random initialization with $\alpha > \alpha_c$ in $\mathcal{O}(\log d)$ iterations and confirm this numerically through extensive simulations. ² We provide a sharp formula

²Note that α_c may or may not coincide with the statistically optimal threshold. In no way do we imply the existence or

for the critical sample complexity α_c above which easy directions are weakly learnable. It is conjectured that no efficient iterative algorithm can succeed for $\alpha < \alpha_c$. The *hardest* multi-index problems are those where α_c diverges, and where none of the directions can be learned from $n = \mathcal{O}(d)$ samples.

- We discuss how interactions among directions can lead to hierarchical learning phenomena, with the hierarchy referring to learning a sequence of growing subspaces. Interestingly, even hard directions can be learned when coupled to easier ones through a hierarchical process, which is reminiscent of the staircase phenomenon for one-pass SGD (Abbe et al., 2023). However, the class of functions that are weakly learnable hierarchically with AMP differs from SGD and is, in particular, considerably larger. We characterise this class of *grand staircase functions* and argue it is the relevant computational complexity class for learning multi-index models.

Finally, the code to reproduce our plots, to run the AMP algorithm, and to deploy state evolution is available on GitHub <https://github.com/SPOC-group/FundamentalLimitsMultiIndex>

Further related work — With its origins on the classical projection pursuit method (Friedman and Tukey, 1974; Friedman and Stuetzle, 1981), there is an extensive literature dedicated to designing and analysing efficient algorithms to train multi-index models models, such as Isotronic Regression for single-index (Brillinger, 1982; Kalai and Sastry, 2009; Kakade et al., 2011) and Sliced Inverse Regression in the multi-index case (Dalalyan et al., 2008; Yuan, 2011; Fornasier et al., 2012; Babichev and Bach, 2018).

The case $p = 1$ has seen a lot of interest recently. In terms of gradient descent, Arous et al. (2021) has shown that if the link function g is known, one-pass SGD achieves weak recovery in $n = \Theta(d^{\ell-1})$ steps, where ℓ , known as the *information exponent*, is the first non-zero Hermite coefficient of the link function g . In the non-parametric setting —where g is unknown— Berthier et al. (2023) has shown that a large-width two-layer neural network trained under one-pass SGD can learn an "easy" single-index target ($\ell = 1$) in $n = \Theta(d)$ steps. This is to be contrasted with full-batch GD, which can achieve weak recovery in $\Theta(1)$ steps with sample complexity $n = \Theta(d)$ even for particular problems with $\ell > 1$ (Dandi et al., 2024) (which is, indeed, the statistical optimal rate (Barbier et al., 2019; Mondelli and Montanari, 2019)). Similar results have also been proven for abstract computational models. Damian et al. (2022) has proven a lower bound $n \geq d^{\max(1, \ell/2)}$ under the Correlational Statistical Query (CSQ) model, comprising algorithms that take queries of the type $\mathbb{E}[y\varphi(\mathbf{x})]$. More recently, Damian et al. (2024) has proven a similar result for the Statistical Query (SQ) model, which allows for more flexible queries of the type $\mathbb{E}[\varphi(\mathbf{x}, y)]$ and hence a lower sample complexity $n \geq d^{\max(1, \kappa/2)}$ with $\kappa \leq \ell$ defining the *generative exponent*. This turns out to be equivalent to the optimal computational weak recovery threshold of (Barbier et al., 2019; Mondelli and Montanari, 2019; Luo et al., 2019; Maillard et al., 2020).

While the situation is less understood, the multicase has also whiteness a surge of recent interest. In particular, it has been used to understand the behavior of gradient descent algorithm in neural networks. For instance, Abbe et al. (2022; 2023) showed that a certain class of *staircase* functions can be learned by large-width two-layer networks trained under one-pass SGD with sample complexity $n = \Theta(d)$. This is in stark contrast to (embedded) s -sparse parities, which require $n \geq d^{s-1}$ samples (Blum et al., 2003). Abbe et al. (2022; 2023) introduced the *leap exponent*, a direction-wise generalisation of the information exponent for multi-index models, and studied the class of *staircase functions* which can be efficiently learned with one-pass SGD. Bietti et al. (2023) showed that under a particular gradient flow scheme preserving weight orthogonality (a.k.a. *Stiefel gradient flow*), training follow a saddle-to-saddle dynamics, with the characteristic time required to escape a saddle given by the leap exponent. Interestingly, it was then shown that the limit discovered in these set of works could be bypassed by slightly different algorithm, for instance by smoothing the landscapes Damian et al. (2023) or reusing batches multi-time Dandi et al. (2024). The latter paper, in particular, showing that gradient descent could learn efficiently a larger class of multi-index models that previously believed to be possible. These findings highlight the need of a strict understanding of the limit learnability of these models.

Our approach to establish the limit of computational learnability is based on the study of the approximate message passing algorithm (AMP). Originating from the cavity method in physics Mézard (1989); Kabashima (2008), AMP Donoho et al. (2009), and its generalized version GAMP Rangan (2011) are powerful iterative algorithm to study these high-dimensional setting. These algorithm are widely believed to be optimal between

absence of a computational-to-statistical gap.

all polynomial algorithms for such high-dimensional problems Zdeborová and Krzakala (2016); Deshpande and Montanari (2015); Bandeira et al. (2018); Aubin et al. (2019); Bandeira et al. (2022). In fact, they are provably optimal among all iterative first-order algorithms Celentano et al. (2020); Montanari and Wu (2022), a very large class of methods that include gradient descent.

While these algorithm were studied in great detail for the single index models, see e.g. Barbier et al. (2019); Aubin et al. (2020b;a), and are at the roots of the spectral method that underline the learnability phase transition in this case Mondelli and Montanari (2019); Maillard et al. (2020), much less is known in the multi-index case, with the exception of Aubin et al. (2019), who showed that particular instances of multi-index models known as *committee machines* can be learned with $n = \mathcal{O}(d)$ samples.

Different from our approach are (Diakonikolas et al., 2020; Goel et al., 2020; Chen et al., 2022), who focused also on peculiar form of the multi-index models (using combination of Relu) and derived worst case bound (in terms of the hardest possible function). Instead, we focus on the typical-case learnability of a given, explicit, multi-index model.

2 Settings and definitions

Using standard notations³, our main focus in this work will be to study subspace identifiability in the class of *Gaussian multi-index models*.

Definition 1 (Gaussian multi-index models). *Given a covariate $\mathbf{x} \sim \mathcal{N}(0, 1/d\mathbf{I}_d)$, we define the class of Gaussian multi-index models as output mappings of the type:*

$$y = g(\mathbf{W}^* \mathbf{x}) \quad (2)$$

where $g : \mathbb{R}^p \rightarrow \mathbb{R}$ denotes the link function and $\mathbf{W}^* \in \mathbb{R}^{p \times d}$ is a weight matrix with i.i.d. rows $\mathbf{w}_k^* \sim \mathcal{N}(0, \mathbf{I}_d)$. Note we allow the map $g : \mathbb{R}^p \rightarrow \mathbb{R}$ to be stochastic i.e $g(\cdot) = \tilde{g}(\cdot, \xi)$ for random variable $\xi \in \mathbb{R}^p$ independent of \mathbf{x} having a fixed dimension-independent law such that $\mathbb{E} [\|\xi\|_2^2] < \infty$.⁴

Given n i.i.d. samples $(\mathbf{x}_i, y_i)_{i \in [n]}$ drawn as per Definition 1, we are interested in investigating the computational bottlenecks of estimating \mathbf{W}^* from the samples $(\mathbf{x}_i, y_i)_{i \in [n]}$. Note that reconstructing \mathbf{W}^* or a permutation of its rows is equivalent from the perspective of the likelihood Equation (2). Therefore, in this work, we will be interested in *weak subspace learnability*, which corresponds to obtaining an estimation of the subspace spanned by \mathbf{W}^* better than a random estimator. This can be defined in an invariant way:

Definition 2 (Weak subspace recovery). *Let $V^* \subset \mathbb{R}^p$ denote a subspace spanned by vectors representing components along \mathbf{W}^* such that each $\mathbf{v} \in V^*$ maps to a vector \mathbf{v}_d in \mathbb{R}^d through the map $\mathbf{v}_d = (\mathbf{W}^*)^\top \mathbf{v}$. Given an estimator $\hat{\mathbf{W}} \in \mathbb{R}^{p \times d}$ of \mathbf{W}^* with $\|\hat{\mathbf{W}}_i\|_F^2 = \Theta(d)$, we have weak recovery of a V^* if:*

$$\inf_{\mathbf{v} \in \mathbb{R}^p, \|\mathbf{v}\|=1} \left\| \frac{\hat{\mathbf{W}}(\mathbf{W}^*)^\top \mathbf{v}}{d} \right\| = \Theta(1). \quad (3)$$

with high probability as $d \rightarrow \infty$.

Our main tool for characterising the computational bottlenecks in the multi-index problem is an *Approximate Message Passing* (AMP, Algorithm 1) acting on $\mathbf{B} \in \mathbb{R}^{d \times p}$ and $\Omega \in \mathbb{R}^{n \times p}$ tailored to our needs:

$$\Omega^t = \mathbf{X} f_t(\mathbf{B}^t) - g_{t-1}(\Omega^{t-1}, \mathbf{y}) \mathbf{V}_t \quad (4)$$

$$\mathbf{B}^{t+1} = \mathbf{X}^T g_t(\Omega^t, \mathbf{y}) + f_t(\mathbf{B}^t) \mathbf{A}_t \quad (5)$$

³We denote by \mathcal{S}_p^+ , the cone of positive-semi-definite matrices in \mathbb{R}^p and by \succ the associated partial ordering. For $\mathbf{M} \in \mathcal{S}_p^+$, we denote by $\sqrt{\mathbf{M}}$ the matrix-square root. $\|\cdot\|$ denotes the operator norm and $\|\cdot\|_F$ the Frobenius norm. For two sequences of scalars $f(d), g(d)$, we use the standard asymptotic notation $f(d) = \Theta(g(d))$ to denote that $c|g(d)| \leq |f(d)| \leq C|g(d)|$ for some constants $0 < c \leq C$ and large enough d . We denote by $f(d) = \mathcal{O}(g(d))$ and $f(d) = \Omega(g(d))$ the one-sided asymptotic bounds $|f(d)| \leq C|g(d)|$ and $c|g(d)| \leq |f(d)|$ respectively.

⁴Technically, our results hold for $\xi \in \mathbb{R}^{p'}$ with $p' = \mathcal{O}(1)$, for example the case of a degenerated noise. But for simplicity of exposition we focus on the $p' = p$ case.

where the denoisers $g_t(\cdot, y_i)$ and $f_t(\cdot)$ are vector-valued mapping applied row-wise on $\omega_i \in \mathbb{R}^p = \Omega_{\cdot i}$ and $\mathbf{b}_i \in \mathbb{R}^p = \mathbf{B}_{\cdot i}$. Here $\hat{\mathbf{W}}^t \in \mathbb{R}^{p \times d} = f_t(\mathbf{B}^t)^\top$ are the estimator of the weights matrix \mathbf{W}^* , $g_t(\Omega^t) \in \mathbb{R}^{n \times p}$ are an estimate of the pre-activations, while \mathbf{A}_t and \mathbf{V}_t are the so-called Onsager terms (see Sec. A).

AMP only involves matrix multiplication by $\mathbf{X} \in \mathbb{R}^{n \times d}$ (and its transpose) and thus belongs to the class of first-order algorithms with linear running time of $\mathcal{O}(nd)$. The key property of AMP is that for well-chosen g_t and f_t (using Bayesian denoisers) it is provably optimal within the class of first-order methods (Celentano et al., 2020). In our case, this require $g_t(\omega, y) = \mathbf{g}_{\text{out}}(y, \omega, \mathbf{V}) \in \mathbb{R}^p$ as in eq. (6), while f_t is just a Gaussian Bayesian denoiser (see Sec. A). Learnability for the optimal AMP thus implies a computational lower bound in the class of first-order methods, including in particular popular machine learning algorithms such as gradient descent (SG). For the Gaussian multi-index estimation problem 1, \mathbf{g}_{out} is given by the optimal denoiser of an effective p -dimensional problem $Y = g(\mathbf{V}^{1/2} \mathbf{Z} + \omega)$ with $\mathbf{Z} \sim \mathcal{N}(\mathbf{0}, \mathbf{I}_p)$, which reads

$$\mathbf{g}_{\text{out}}(y, \omega, \mathbf{V}) = \mathbb{E}[\mathbf{Z}|Y = y] = \frac{\int_{\mathbb{R}^p} d\mathbf{z} e^{-\frac{1}{2}(\mathbf{z}-\omega)^\top \mathbf{V}^{-1}(\mathbf{z}-\omega)} P(y|\mathbf{z}) \mathbf{V}^{-1}(\mathbf{z}-\omega)}{\int_{\mathbb{R}^p} d\mathbf{z} e^{-\frac{1}{2}(\mathbf{z}-\omega)^\top \mathbf{V}^{-1}(\mathbf{z}-\omega)} P(y|\mathbf{z})}, \quad (6)$$

where the conditional expectation is defined through the output channel $Y = g(\mathbf{V}^{1/2} \mathbf{Z} + \omega)$. For stochastic mappings $g(\cdot) = g(\cdot, \xi)$, the expectation is w.r.t both Z, ξ conditioned on Y . Our results rely on the following assumption on the above denoiser, translating to weak assumptions on g, ξ :

Assumption 1. (a) $\mathbf{g}_{\text{out}} : \mathbb{R}^{p^2+p+1} \rightarrow \mathbb{R}^p \in \mathcal{C}^2$. (b) the mapping $\hat{\mathbf{g}}_{\text{out}} : \mathbb{R}^{p+p'} \rightarrow \mathbb{R}^p$ defined by $\hat{\mathbf{g}}_{\text{out}}(\mathbf{h}, \xi) = \mathbf{g}_{\text{out}}(\tilde{g}(\mathbf{h}, \xi), \omega, \mathbf{V})$ is pseudo-Lipschitz of finite-order for all $\omega, \mathbf{V} \in \mathbb{R}^p, \mathbb{R}^{p \times p}$. Here, $\xi \in \mathbb{R}^{p'}$ denotes independent noise satisfying $\mathbb{E}[\|\xi\|^2] < \infty$ as per Def. 1.

The above denoiser can also be derived as an exact high-dimensional approximation of the Belief Propagation (BP) algorithm for the estimation of the marginals of the Bayesian posterior distribution:

$$p(\mathbf{W}|\mathbf{X}, \mathbf{y}) \propto \prod_{i=1}^n \delta(y_i - g(\mathbf{W}\mathbf{x}_i)) \prod_{k=1}^p \mathcal{N}(\mathbf{w}_k|\mathbf{0}, \mathbf{I}_d). \quad (7)$$

The Bayes-AMP algorithm was derived for Gaussian multi-index models by Aubin et al. (2019), although it has been analysed only for the particular link function $g(\mathbf{z}) = \text{sign}(\sum_{k \in [p]} \text{sign}(z_k))$, known as the *committee machine*. Our goal in this work is to leverage Algorithm 1 in order to provide a sharp classification of which link functions g are computationally challenging to learn. Our analysis is based on two remarkable properties that make AMP a particularly useful tool for studying high-dimensional estimation. The first property is that for any $t = \Theta(1)$, in the high-dimensional limit $d \rightarrow \infty$ the performance of AMP can be tracked without actually running the algorithm. This result, known as *state evolution*, makes AMP mathematically tractable in high-dimensions (Bayati and Montanari, 2011). The second property is its optimality with respect to Bayesian estimation (see SI, A). For multi-index models, the state evolution equations were derived by Aubin et al. (2020b) and rigorously proven by Gerbelot and Berthier (2023). It provides, in particular, an exact characterization of the asymptotic overlaps and prediction error:

Lemma 2.1 (State evolution (Aubin et al., 2019; Gerbelot and Berthier, 2023)). *Let $(\mathbf{x}_i, y_i)_{i \in [n]}$ denote n i.i.d. samples from the multi-index model eq.(1). Run AMP from random initialization $\hat{\mathbf{W}}^0 \in \mathbb{R}^{p \times d}$ with $\hat{\mathbf{w}}_k^0 \stackrel{i.i.d.}{\sim} \mathcal{N}(\mathbf{0}, \mathbf{I}_d)$. Denote by $\hat{\mathbf{W}}^t$ the resulting estimator at time $0 \leq t \leq T$. Then, in the high-dimensional limit $n, d \rightarrow \infty$ with fixed ratio $\alpha = n/d$, constant p & any finite time T , the limiting overlaps satisfy:*

$$\frac{1}{d} \hat{\mathbf{W}}^t \hat{\mathbf{W}}^{t\top} \xrightarrow{P} \mathbf{M}^t, \quad \frac{1}{d} \hat{\mathbf{W}}^t \mathbf{W}^{*\top} \xrightarrow{P} \mathbf{M}^t, \quad (8)$$

with \mathbf{M}^t satisfying the state evolution equations from initial condition \mathbf{M}^0 iterated with $\mathbf{M}^{t+1} = F(\mathbf{M}^t)$:

$$F(\mathbf{M}^t) = G\left(\alpha \mathbb{E}\left[\mathbf{g}_{\text{out}}\left(Y^t, \sqrt{\mathbf{M}^t} \xi, \mathbf{I}_p - \mathbf{M}^t\right)^{\otimes 2}\right]\right). \quad (9)$$

where $G(\mathbf{X}) = (\mathbf{I}_p + \mathbf{X})^{-1} \mathbf{X}$ and the expectation is taken over the following effective process

$$Y^t = g\left((\mathbf{I}_p - \mathbf{M}^t)^{1/2} \mathbf{Z} + \mathbf{M}^{t/2} \xi\right), \quad (10)$$

with $\mathbf{Z}, \boldsymbol{\xi} \sim \mathcal{N}(0, \mathbf{I}_p)$ independently from \mathbf{Z} . The asymptotic mean-squared error on the label prediction is then given by:

$$\mathbb{E}_{\mathbf{x}, y} \left[\left(y - g \left(\hat{\mathbf{W}}^t(\mathbf{X}, \mathbf{y}) \mathbf{x} \right) \right)^2 \right] \xrightarrow{P} \mathbb{E}[(Y^t - g(\mathbf{Z}))^2],$$

where the expectation is taken over the effective estimation process eq.(10) and \xrightarrow{P} denotes convergence in probability w.r.t $\mathbf{X}, \mathbf{y}, \hat{\mathbf{W}}^0$ as $n, d \rightarrow \infty$.

3 The trivial subspace ($\alpha_c = 0$)

The state evolution Equation (9) maps the problem of characterising the computational bottlenecks of first-order methods for high-dimensional Gaussian multi-index models to the study of the deterministic, p -dimensional dynamical system $\mathbf{M}^{t+1} = F(\mathbf{M}^t)$. A starting point is identifying its fixed points and their basins of attraction. In the absence of any prior information on \mathbf{W}^* aside from its distribution, one cannot do better than taking $\hat{\mathbf{w}}_k^{t=0} \sim \mathcal{N}(\mathbf{0}, \mathbf{I}_d)$ with $k \in [p]$ independently at random from the prior. With high-probability, at initialization, the elements of the overlap matrix $1/d \hat{\mathbf{W}}^0 \mathbf{W}^{*\top}$ are $\Theta(d^{-1/2})$ element-wise. The asymptotic overlap for an uninformed initial condition is thus $\mathbf{M}^0 = 0$, a null-rank matrix. If $\mathbf{M}^0 = 0$ is not a fixed point, then $\mathbf{M}^1 \succ 0$, implying the weak recovery of a subspace of dimension $k = \text{rank}(\mathbf{M}^1) > 0$ with just a *single step of AMP*.

Lemma 3.1 (Existence of uninformed fixed point). $\mathbf{M} = \mathbf{0} \in \mathbb{R}^{p \times p}$ is a fixed point of Equation (9) if and only if the following condition holds almost surely over Y :

$$\mathbf{g}_{\text{out}}(Y, \boldsymbol{\omega} = \mathbf{0}, \mathbf{V} = \mathbf{I}_p) = \mathbb{E}[\mathbf{Z}|Y] = \mathbf{0}, \quad (11)$$

As long as the conditional expectation above is not zero almost surely, then AMP weakly learns a non-empty subspace immediately in the first iteration for any number of samples $n = \Theta(d)$. For this reason, we refer to this subspace as a *trivial subspace*:

Definition 3 (Trivial subspace). We define $H_T^* \subseteq \mathbb{R}^p$ as the subspace spanned by $\mathbf{v} \in \mathbb{R}^p$ such that the following holds almost surely over $Y = g(\mathbf{Z})$ with $\mathbf{Z} \sim \mathcal{N}(\mathbf{0}, \mathbf{I}_p)$:

$$\mathbf{g}_{\text{out}}(Y, \mathbf{0}, \mathbf{I}_p)^\top \mathbf{v} = \lim_{d \rightarrow \infty} \mathbb{E}[\langle \mathbf{v}^\top \mathbf{W}^*, \mathbf{x} \rangle | y = Y] = 0, \quad (12)$$

where the expectation is w.r.t the joint measure $p(\mathbf{x}, y)$ defined in Def. 1 eq.(10). The trivial subspace T^* is the orthogonal complement of H_T^* .

Theorem 3.2. For any $\alpha > 0$, with high-probability as $d \rightarrow \infty$, the AMP algorithm with the Bayes-optimal choice of f_t, g_t recovers T^* as per Definition 2 in a single iteration.

Note that for single-index models ($p = 1$), the condition in Equation (11) reduces to the one derived by (Mondelli and Montanari, 2019; Barbier et al., 2019; Maillard et al., 2020). Interestingly, this is *exactly* the same condition appearing in Damian et al. (2024) for weak learnability of single-index models in the SQ model; see eq. (3) therein. To make Lemma 3.1 concrete, let us look at a few examples (A detailed derivation of these examples is presented in Appendix F):

1. For single-index models ($p = 1$), T^* is one dimensional if and only if g is non-even, e.g. $g(z) = \text{He}_3(z)$. This follows from requiring that $g_{\text{out}}(y, 0, 1) \neq 0$ for at least one value of y . In particular, on any open interval where g_{out} is invertible we have $g_{\text{out}} = g^{-1}$.
2. For a linear multi-index model, $g(\mathbf{z}) = \sum_{i=1}^p z_i$, T^* is spanned by $\mathbf{1}_p \in \mathbb{R}^p$ (all-one vector).
3. For a committee $g(\mathbf{z}) = \sum_{i=1}^p \text{sign}(z_i)$, the trivial subspace T^* is again 1-d, spanned by $\mathbf{1} \in \mathbb{R}^p$.
4. For monomials $g(\mathbf{z}) = z_1 \dots z_p$, the trivial subspace T^* is non-empty if and only if $p = 1$.
5. For leap one staircase functions (Abbe et al., 2023):

$$g(\mathbf{z}) = z_1 + z_1 z_2 + z_1 z_2 z_3 + \dots \quad (13)$$

The trivial subspace is $T^* = \mathbb{R}^p$ and is spanned by the canonical basis. In other words, AMP learns all the directions with a *single step* for any $\alpha > 0$.

Lemma 3.1 can also be related to computational models based on queries, such as SQ learning (Kearns, 1998): the denoiser \mathbf{g}_{out} can indeed be interpreted as a non-linear transformation on the labels $y \mapsto \mathbf{g}_{\text{out}}(y, \mathbf{0}, \mathbf{I}_p)$. From this perspective, the statement on the condition for the existence of a non-empty trivial subspace (12) translates to the condition $\mathbb{E} [\mathbf{g}_{\text{out}}(y, \mathbf{0}, \mathbf{I}_p)^\top \mathbf{v} \langle \mathbf{v}^\top \mathbf{W}^*, \mathbf{x} \rangle] = \mathbb{E} [\mathbb{E}[\langle \mathbf{v}^\top \mathbf{W}^*, \mathbf{x} \rangle | Y = y]^2] \neq 0$ where $\mathbf{v} \in T^*$. The left-hand side can be seen as a statistical query of the type $\mathbb{E}[\varphi(y)\psi(x)]$ with label pre-processing $\varphi = \mathbf{g}_{\text{out}}$. The fact that this linear correlation in the transformed labels is non-vanishing implies that one can weakly recover \mathbf{v} through a tailored spectral method (Mondelli and Montanari, 2019; Luo et al., 2019). In fact the denoiser \mathbf{g}_{out} is the optimal such transformation in the sense that when \mathbf{g}_{out} fails to obtain a linear correlation along \mathbf{v} , i.e when $\mathbf{v} \in H^*$, then no transformation can:

Lemma 3.3. $\mathbf{v} \in H^*$ if and only if for any measurable transformation $\mathcal{T} : \mathbb{R} \rightarrow \mathbb{R}$:

$$\lim_{d \rightarrow \infty} \mathbb{E} [\mathcal{T}(y) \langle \mathbf{v}^\top \mathbf{W}^*, \mathbf{x} \rangle] = 0. \quad (14)$$

Note that the expectation is with respect to the distribution of the labels y (not the effective problem). Equivalently, $\mathbf{v} \in T^*$ if and only if there exists a transformation such that $\lim_{d \rightarrow \infty} \mathbb{E} [\mathcal{T}(y) \langle \mathbf{v}^\top \mathbf{W}^*, \mathbf{x} \rangle] \neq 0$.

Remarks on GD — The characterization of H^* and T^* allows us to contrast the (optimal) performance of AMP with that of gradient-descent based methods on neural nets: First, note that when T^* is empty, then $\mathbb{E} [\mathcal{T}(y) \langle \mathbf{v}^\top \mathbf{W}^*, \mathbf{x} \rangle] = 0$ for all $\mathbf{v} \in \mathbb{R}^p$. This is precisely the condition for the generative exponent (Damian et al., 2024) being strictly larger than 1. This implies that one-pass SGD —even after applying any transformation \mathcal{T} — fails to obtain weak recovery with $\mathcal{O}(d)$ samples (see Thms. 1.3 and 1.4 in Arous et al. (2021)). The converse question is interesting: For non-empty T^* , can GD recover T^* with just $\mathcal{O}(d)$ steps? In the absence of any transformations of the labels, this remains false for online SGD (Arous et al., 2021; Abbe et al., 2022), unless the *information* exponent of g is 1. The situation is different when reusing batches: Dandi et al. (2024) indeed showed that full batch GD on a two-layer neural network implicitly applies transformation \mathcal{T} to the labels. The learnable subspace in two iterations with $\mathcal{O}(d)$ sample complexity then *exactly coincides* with that of T^* in Lemma 3.3, up to the restriction to polynomial transformations. A two-layer network with re-use of batches can thus recover the full trivial subspace efficiently for any $\alpha > 0$.

4 Phase transitions ($\alpha_c > 0$)

When the trivial subspace T^* from Def. 3 is empty, $\mathbf{M} = \mathbf{0}$ is a fixed point of state-evolution, thus AMP starting from random initialization fails to recover any subspace of \mathbf{W}^* in any *finite* number of steps. However, there may exist directions where recovery requires only an infinitesimal additional side-information. To contrast with the trivial subspace, we refer to the directions learnable for arbitrarily small side-information as the *easy directions*.

The learnability of easy subspaces is characterized by AMP’s stability, which crucially depends on the sample complexity $\alpha = n/d$. The stability of $\mathbf{M} = \mathbf{0}$ is studied by linearising the state evolution (9) around $\delta\mathbf{M}$ with $\|\delta\mathbf{M}\| \approx 0$

$$F(\mathbf{M}) \approx \alpha \mathcal{F}(\delta\mathbf{M}) + \mathcal{O}(\|\delta\mathbf{M}\|^2),$$

where $\mathcal{F}(\delta\mathbf{M})$ is a linear operator on the cone \mathcal{S}_p^+ of PSD matrices of dimension p :

$$\mathcal{F}(\mathbf{M}) := \mathbb{E}_Y [\partial_{\omega} \mathbf{g}_{\text{out}}(Y, \mathbf{0}, \mathbf{I}_p) \mathbf{M} \partial_{\omega} \mathbf{g}_{\text{out}}(Y, \mathbf{0}, \mathbf{I}_p)^\top]. \quad (15)$$

The above linearization demarcates a threshold on α , below which the AMP remains stable:

Lemma 4.1. (Stability of the uninformed fixed point). *If $\mathbf{M} = \mathbf{0} \in \mathbb{R}^{p \times p}$ is a fixed point, then it is an unstable fixed point of Equation (9) if and only if $\|\mathcal{F}(\mathbf{M})\|_F > 0$ and $n > \alpha_c d$, where the critical sample complexity α_c is:*

$$\frac{1}{\alpha_c} = \sup_{\mathbf{M} \in \mathbb{R}^{p \times p}, \|\mathbf{M}\|_F = 1} \|\mathcal{F}(\mathbf{M})\|_F, \quad (16)$$

with $\|\cdot\|_F$ denoting the Frobenius norm. Moreover, if $\mathcal{F}(\mathbf{M}) \neq 0$, there exists at-least one $\mathbf{M}^* \neq 0 \in \mathcal{S}_p^+$ achieving the above supremum. While if $\mathcal{F}(\mathbf{M}) = 0$, then $\mathbf{M} = \mathbf{0}$ is a stable fixed point for any $n = \Theta(d)$.

The above result follows from a generalization of the Perron-Frobenius theorem to the cone \mathcal{S}_p^+ ; see Appendix D.3 for a proof. Analogously, the operator $\mathcal{F}(\mathbf{M})$ allows us to define the stability threshold along a specific direction $\mathbf{v} \in \mathbb{R}^p$. We define the *easy subspace* as containing the directions where $\mathbf{M} = \mathbf{0}$ becomes unstable for some $\alpha < \infty$:

Definition 4 (Easy subspace E^*). *Let H_E^* be the subspace spanned by directions $\mathbf{v} \in \mathbb{R}^p$ such that:*

$$\mathbf{v}^\top \partial_{\boldsymbol{\omega}} \mathbf{g}_{\text{out}}(Y, \boldsymbol{\omega} = \mathbf{0}, \mathbf{V} = \mathbf{I}_p) \mathbf{v} = 0, \quad (17)$$

almost surely over Y . We define the easy subspace E^ as the orthogonal complement of H_E^* .*

Modeling side information as additional observations:

$$\mathbf{S} = \sqrt{\lambda} \mathbf{W}^* + \sqrt{1 - \lambda} \mathbf{Z}, \quad (18)$$

where $\mathbf{Z} \in \mathbb{R}^{p \times d}$ has independent entries $Z_{ij} \sim \mathcal{N}(0, 1)$, we can now state our main theorem:

Theorem 4.2. *Let $\mathbf{M}_d^t := 1/d \hat{\mathbf{W}}^t \mathbf{W}^{*\top}$ denote the model-target overlap matrix at any finite time t . Suppose that $T^* = 0$ and consider the AMP algorithm with the Bayes-optimal choice of f_t, g_t . Then, with high probability as $d \rightarrow \infty$:*

- (i) *For $\alpha \geq \alpha_c$, $\exists \delta > 0$ such that for any sufficiently small λ , $\mathbf{M}_d^t \succ \delta \mathbf{M}^*$ for $t = \mathcal{O}(\log^{1/\lambda})$, where \mathbf{M}^* is any of the extremizers defined in Lemma 4.1. Furthermore, there exists an $\alpha \geq \alpha_c$ and a $\delta > 0$ such that $\mathbf{M}_d^t \succ \delta \mathbf{M}_{E^*}$ in $t = \mathcal{O}(\log^{1/\lambda})$ iterations, where $\mathbf{M}_{E^*} \in \mathcal{S}_p^+$ spans E^* .*
- (ii) *For $\alpha < \alpha_c$ however, $\mathbf{M}_d^t = \mathbf{0}$ is asymptotically stable i.e. there exist constants $\lambda' < 1$ and $C > 0$ such that for $\lambda < \lambda'$, $\sup_{t \geq 0} \|\mathbf{M}_d^t\| \leq C\sqrt{\lambda}$.*

Concretely, this implies that for $\alpha < \alpha_c$, not only does AMP fail to find any pertinent directions, but it also fails to improve on the small side-information. For $\alpha > \alpha_c$, however, AMP will develop a growing overlap along a non-empty subspace starting with *arbitrarily small* (but finite) side information. Based on the optimality of AMP amongst first-order methods for any finite number of iterations (Celentano et al., 2020; Montanari and Wu, 2022), α_c thus marks the onset of *computational phase transition* (see S.I. E) for weak learnability in the first-order methods class.

Note that in Thm. 4.2 the side information snr $\lambda > 0$ can be arbitrarily small, but must remain $\mathcal{O}(1)$. Based on a vast array of evidence from statistical physics literature, we are actually claiming a *stronger result*, and believe the following conjecture to be exact:

Conjecture 1. *AMP initialized randomly will find a finite overlap with the easy directions for $\alpha > \alpha_c$ in $\mathcal{O}(\log d)$ steps, without side information.*

This can be justified by the heuristic $\lambda = \mathcal{O}(1/\sqrt{d})$ (as this is the scaling of the correlation with the ground truth at initialization) in Thm. 4.2. While is not strictly covered by the state evolution theorem that allow only a finite number of steps, it is however well obeyed in practice in our simulations (see Fig.2) and it is a well known observation in many message-passing works that AMP (or belief propagation) find the fixed point after few iterations from a random start (see e.g. Decelle et al. (2011); Zdeborová and Krzakala (2016); Barbier et al. (2019)).

A rigorous proof, though, remain a difficult open problem that require a non-asymptotic control of the AMP state evolution, see (Rush and Venkataraman, 2018; Li and Wei, 2022; Li et al., 2023) for some recent progress in the context of \mathbb{Z}_2 synchronization where the convergence from random start has been established, corroborating the heuristic identification $\lambda = \mathcal{O}(1/\sqrt{d})$ in this case. An alternative possible strategy to provide a recovery algorithm in $\mathcal{O}(\log(d))$ steps would be to follow (Krzakala et al., 2013; Maillard et al., 2022) and linearize AMP to reach a power iteration method (with a matrix similar to the one discussed in Lemma 3.3) so that the resulting operator can be studied with random matrix theory (Guionnet et al., 2023; Mondelli and Venkataraman, 2021), as was done for the single-index model in (Mondelli and Montanari, 2019; Lu and Li, 2020; Maillard et al., 2022). We leave these, and the proof of conjecture 1, open for further studies.

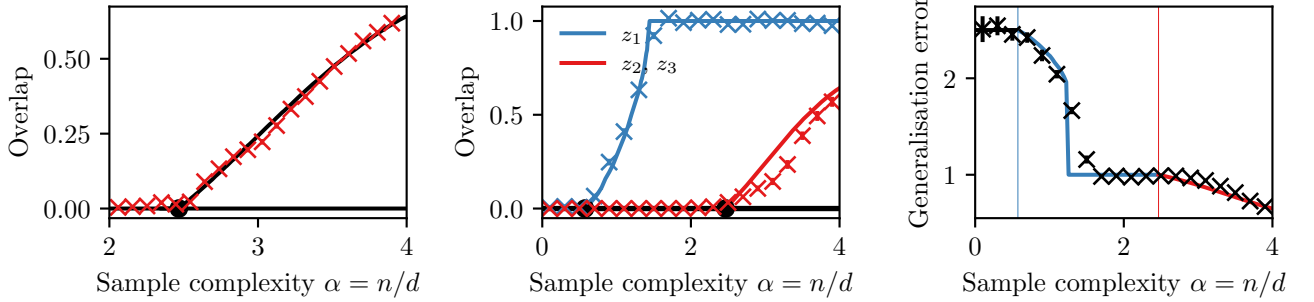


Figure 1: Weak learnability phase transitions for $g(z_1, z_2) = \text{sign}(z_1 z_2)$ (left) and $g(z_1, z_2, z_3) = z_1^2 + \text{sign}(z_1 z_2 z_3)$ (center and right). Given the permutation symmetry in the models, we display the optimal permutation of the overlap matrix elements reached by AMP. **(Left):** Overlaps with the two directions $1/2(M_{11} + M_{22})$ as a function of the sample complexity $\alpha = n/d$, with the phase transition at $\alpha_c = \pi^2/4$. The solid black line is the asymptotic theory from state evolution while crosses are averages over 72 AMP runs with $d = 500$. **(Center):** Overlaps with the first direction $|M_{11}|$ (blue), and with the second and third one $1/2(M_{22} + M_{33})$ (red) as a function of the sample complexity $\alpha = n/d$. Solid lines are the state evolution curves Equation (9), and crosses/dots AMP runs with $d = 500$ averaged over 72 seeds. All other overlaps are zero (black). The two black dots indicate the critical thresholds at $\alpha_1 \approx 0.575$ and $\alpha_2 = \pi^2/4$. **(Right)** Corresponding generalization error as a function of $\alpha = n/d$. The figure can be reproduced using the code provided (See also Appendix G).

The expression for the weak recovery threshold Eq.(16) in Lemma 3.1 allows to generalise the single-index expression from (Mondelli and Montanari, 2019; Barbier et al., 2019; Maillard et al., 2020). Indeed, for $p = 1$, we have $\partial_\omega g_{\text{out}}(y, 0, 1) = \mathbb{E}[\text{He}_2(Z)|Y = y]$, and therefore $\alpha_c = \mathbb{E}_Y [\mathbb{E}[\text{He}_2(Z)|Y]^2]^{-1}$ or equivalently

$$\frac{1}{\alpha_c} = \int_{\mathbb{R}} dy \frac{\left[\int_{\mathbb{R}} \frac{dz}{2\pi} e^{-\frac{1}{2}z^2} (z^2 - 1) P(y|z) \right]^2}{\int_{\mathbb{R}} \frac{dz}{2\pi} e^{-\frac{1}{2}z^2} P(y|z)} \quad (19)$$

which is exactly the threshold in (Barbier et al., 2019; Mondelli and Montanari, 2019; Lu and Li, 2020; Maillard et al., 2022; Damian et al., 2024).

We now illustrate Lemma 4.1 in a two examples of interest:

(i) **The monomial** $g(\mathbf{z}) = z_1 \dots z_p$ with $p > 1$ can always be learned with $\alpha > \alpha_c(p)$ large enough (Chen and Meka, 2020). For instance, we have $\alpha_c(2) \approx 0.5937$, $\alpha_c(3) \approx 3.725$ and $\alpha_c(4) \approx 4.912$. In Appendix F we derive an analytical formula for $\alpha_c(p)$ for arbitrary p , and show that $\alpha_c(p) \sim p^{1.2}$ for large p .

(ii) The embedding of the **sparse parity functions**:

$$g(\mathbf{z}) = \prod_{k=1}^p \text{sign}(z_k). \quad (20)$$

As this is invariant under permutations of the indices, Lemma 4.1 implies the existence of a computational phase transition. In S.I. Sec.F.3 we compute analytically the critical value $\alpha_c(p)$: $p=1$ is equivalent to phase retrieval and $\alpha_c(1) = 1/2$. For $p=2$, we show that $\alpha_c(2) = \pi^2/4$, while $\alpha_c(p) = +\infty$ for $p \geq 3$. This is illustrated in Fig.1 (left) for 2-sparse parity.

The sparse-parity function is a classic example of a computationally hard function in theoretical computer science (Blum et al., 1994; 2003).⁵ Therefore, it should come as no surprise that $\alpha_c(p) = \infty$ for $p \geq 3$, providing a concrete example of what a hard subspace (i.e. that cannot be learned with $n = \Theta(d)$ samples) looks like for AMP. Similar to the discussion of trivial directions in Lemma 3.3, we can invoke optimality of AMP to translate our result on the optimal denoiser $y \mapsto \mathbf{g}_{\text{out}}(y, \mathbf{0}, \mathbf{I}_p)$ to a statement for queries on general label pre-processing transformations:

⁵Noiseless parity is actually efficiently learnable by Gaussian elimination (Blum et al., 1994). Here we consider computational efficiency in a noise-tolerant sense.

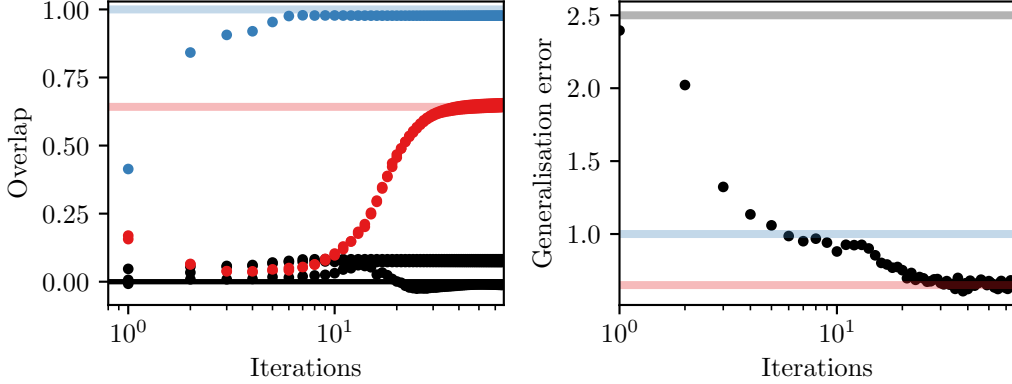


Figure 2: Trajectories of a single finite-size run of AMP with $d = 500$ at $\alpha = 4$ for $g(z_1, z_2, z_3) = z_1^2 + \text{sign}(z_1 z_2 z_3)$. (Left) Evolution of the overlaps. We display M_{11} in blue, $1/2(M_{22} + M_{33})$ in red, and the off-diagonal overlaps in black. (Right) Evolution of the generalisation error.

Lemma 4.3. *For any $\mathbf{v} \in H_E^*$ and any measurable transformation $\mathcal{T} : \mathbb{R} \rightarrow \mathbb{R}$ we have*

$$\lim_{d \rightarrow \infty} \mathbb{E} [\mathcal{T}(y) \text{He}_2(\langle \mathbf{v}^\top \mathbf{W}^*, \mathbf{x} \rangle)] = 0. \quad (21)$$

Note that the expectation is with respect to the distribution of the labels y (not the effective problem from eq.(10)).

Remarks on GD — Analogous to Lemma 3.3, Lemma 4.3, implies that the condition T^*, E^* being empty (i.e. $\alpha_c = \infty$) is equivalent to the generative exponent (Damian et al., 2024) being strictly larger than 2. The results in Arous et al. (2021); Abbe et al. (2023) then imply that even after applying any transformation to the output (as allowed in SQ) online-SGD requires at least $\Omega(d^2)$ samples to achieve weak-recovery, since online-SGD with squared loss requires $\Omega(d^{\kappa-1})$ samples/iterations for weak-recovery of a target function with leap/information exponent κ (Theorems 1.3 and 1.4 in Arous et al. (2021)). Furthermore, for single-index models satisfying the condition in Lemma 4.3 (i.e $\alpha_c = \infty$), the SQ lower-bound predicts a sample complexity requirement of at-least $\Omega(d^{3/2})$ (Damian et al., 2024). Learning such functions with $\mathcal{O}(d)$ samples is thus conjectured to be algorithmically-hard.

It is again a natural question to ask for non-empty E^* , how many samples and iterations do neural networks trained with GD require for achieving weak-recovery. In the absence of label transformations, weak-recovery along E^* requires $\Omega(d^2)$ unless the information exponent is at-most 2 (Arous et al., 2021; Abbe et al., 2023). However, in the presence of transformations, the sample complexity for weak-recovery along E^* can be reduced to $d \text{polylog}(d)$. Chen et al. (2022) already showed that any polynomial can be learned with $d \text{polylog}(d)$ iterations using an SQ algorithm. More-recently, (Arnaboldi et al., 2024; Lee et al., 2024) suggested that E^* can be recovered in $d \text{polylog}(d)$ steps through modified gradient-based algorithms re-using data. It remains an open question, however, to see if $\alpha_d d$ data are enough for an agnostic GD approach.

5 The grand staircase

The present classification of *trivial*, *easy* or *hard* directions, based upon the notion of weak learnability, does not say what can be learned *after* a given subspace is learned. We now address this question. Suppose that the estimator $\hat{\mathbf{W}}^t$ has developed an overlap along a subspace belonging to the span of \mathbf{W}^* , resulting in a non-zero overlap $\mathbf{M}^t \succ 0$. From that point, the main difference with respect to the previous discussion is that the variable $\boldsymbol{\omega}$ in the linear operator \mathcal{F} defined in eq.(15) becomes non-zero (since it is distributed as $\boldsymbol{\omega} = \sqrt{\mathbf{M}}\boldsymbol{\xi}$). Crucially, this changes the span of $\mathcal{F}(\mathbf{M})$ and hence the stability condition in Lemma 4.1. In particular, as we show next, learning some directions might facilitate learning larger subspaces. This is

reminiscent of the specialisation transition in committee machines (Saad and Solla, 1996; Aubin et al., 2020b) and of the staircase for SGD (Abbe et al., 2022):

Definition 5. Let $U \subset \mathbb{R}^p$. We define $H_T^*(U)$ to be the subspace spanned by $\mathbf{v} \in U^\perp$ such that

$$\mathbf{v}^\top \mathbf{g}_{\text{out}}(Y, \sqrt{\mathbf{M}_U} \boldsymbol{\xi}, \mathbf{I} - \sqrt{\mathbf{M}_U}) = 0 \quad (22)$$

almost surely over $\boldsymbol{\xi} \sim \mathcal{N}(\mathbf{0}, \mathbf{I}_p)$ and Y for any $\mathbf{M}_U \in \mathcal{S}_p^+$ such that $\text{span}(\mathbf{M}_U) = U$. We define the “trivially-coupled” subspace T_U^* for U as the orthogonal complement of $H_T^*(U)$.

Analogously, let $H_E^*(U)$ be the subspace spanned by directions $\mathbf{v} \in U^\perp$ such that

$$\mathbf{v}^\top \partial_{\boldsymbol{\omega}} \mathbf{g}_{\text{out}}(Y, \sqrt{\mathbf{M}_U} \boldsymbol{\xi}, \mathbf{I} - \sqrt{\mathbf{M}_U}) \mathbf{v} = 0 \quad (23)$$

almost surely over $\boldsymbol{\xi}$ and Y for any $\mathbf{M}_U \in \mathcal{S}_p^+$ such that $\text{span}(\mathbf{M}_U) = U$.

When \mathbf{M}_U is additionally a fixed point of \mathcal{F}_M , one can linearise \mathcal{F}_M along the orthogonal complement of U . We define the easy-coupled subspace E_U^* for U as the orthogonal complement of $H_E^*(U)$. Next, suppose that $\mathbf{M}_U \in \mathcal{S}_p^+$ with $\text{span}(\mathbf{M}_U) = U$ is a fixed-point of \mathcal{F}_M . Let \mathcal{F}_{M_U} denote the linearization of $F(\mathbf{M})$ along the orthogonal complement U^\perp at $\mathbf{M} = \mathbf{M}_U$. We define the grand staircase threshold $\alpha_{gst}(\mathbf{M}_U)$ at $\mathbf{M} = \mathbf{M}_U$ as $\alpha_{gst}(\mathbf{M}_U) = (\sup_{\mathbf{M}^\perp \in U^\perp} \|\mathcal{F}_{M_U}(\mathbf{M}^\perp)\|_F)^{-1}$.

The definitions above generalise the notions of *trivial* and *easy* subspaces in Def. 3 & 4 conditionally on a subspace U that has been previously learned, and characterise the directions whose recovery is enabled upon learning the subspace U . Concretely, upon developing an initial overlap along U , the directions in T_U^*, E_U^* can be recovered analogous to the recovery of T^*, E^* in Theorems 3.2, 4.2. For brevity, we focus the present discussion on the recovery of E_U^* with vanishing side information, and discuss settings involving the recovery of T_U^* in Appendix C.

Proposition 5.1. (informal) Let $U \subseteq \mathbb{R}^p$ be a subspace such that E_U^* is non-empty. Consider AMP iterates with the Bayes-optimal choice of f_t, g_t for sufficiently small $\lambda > 0$. Suppose that $\mathbf{M}_d^t := {}^{1/d} \hat{\mathbf{W}}^t \mathbf{W}^{*\top}$ is an approximate fixed point of $F(\mathbf{M})$ in Equation (9) such that $\mathbf{M}_d^t \approx \mathbf{M}_U$ where M_U spans U . Then:

- For $\alpha > \alpha_{gst}(\mathbf{M}_U)$, AMP recovers $M_{M_U}^*$ in additional $\mathcal{O}(\log \frac{1}{\lambda})$ steps for arbitrarily small λ , where $M_{M_U}^*$ denotes any matrix in \mathcal{S}_p^+ achieving the supremum $\sup_{\mathbf{M}^\perp \in U^\perp} \|\mathcal{F}_{M_U}(\mathbf{M}^\perp)\|_F$ as per Definition (5).
- For $\alpha < \alpha_{gst}(\mathbf{M}_U)$ and sufficiently small λ , AMP remains at the approximate fixed point \mathbf{M}_U and fails to gain weak-recovery along U^\perp .

When the easy subspace E^* defined by Def. 4 and $E_{E_U^*}^*$ are non-empty, we further show in S.I. D.6 that for large enough $\alpha \geq \alpha_c$ AMP recovers E_U^* by first reaching an approximate fixed point spanning E^* and subsequently “escaping” along $E_{E_U^*}^*$ as described above. A concrete example of a function displaying this phenomenon is a linear combination between *hard* parity function and an *easy* polynomial:

$$g(z_1, z_2, z_3) = z_1^2 + \text{sign}(z_1 z_2 z_3) \quad (24)$$

The sign part is a sparse parity with $p = 3$, which cannot be learned with $n = \Theta(d)$ samples, but the quadratic polynomial z_1^2 component in the function allows weak-recovery of the first component i.e. $U = (1, 0, 0)$ as long as $\alpha > 1/2$. Hence, conditionally on U the effective multi-index model becomes $\text{sign}(z_2 z_3)$, which as discussed in Sec.4 is an *easy* function. Figure 1 illustrates this: first, z_1 is learned at $\alpha_1 \approx 0.575$. Then, for larger value when $\alpha > \alpha_2$, all directions are learned (see figure 1). Knowing z_1 makes the *hard* 3-parity an *easy* 2-parity problem.

It is easy to construct a multi-index model where AMP will iterate over any number of such plateaus. For instance, consider the model:

$$g(\mathbf{z}) = z_1^2 + \text{sign}(z_1 z_2 z_3) + \text{sign}(z_3 z_4 z_5) + \dots \quad (25)$$

After the first plateau to learn z_1 , there will be one for z_2 and z_3 , then for z_4, z_5 . Another example (see Fig. 3 in the S.I.) is the neural net target $g(z_1, z_2, z_3) = \text{sign}(z_1) + \text{sign}(z_2) + \text{sign}(z_3)$. At first only the one-dimensional direction spanned by $z_1 + z_2 + z_3$ is learned for any $\alpha > 0$. This is simply a linear approximation of the function.

Only at $\alpha \approx 4.3$ does the network learns the other directions. Known as the *the specialisation transition*, this provide a very early example of such sequential learning (Saad and Solla, 1996; Aubin et al., 2020a).

We can characterize a sequence of growing subspaces that AMP recovers iteratively, with vanishing side information, for large enough α , as follows:

Definition 6. Let $E_1^* = E^* \cup T^*$, and inductively define for $k \in \mathbb{N}$:

$$E_{k+1}^* = E_k^* \cup E_{E_k^*}^* \cup T_{E_k^*}^* \quad (26)$$

The dimensionality of the subspaces in the above sequence is non-decreasing and therefore, $\exists k$ such that $E_{E_k^*}^* = \emptyset$. We denote this maximal subspace by E_{gst}^* and say that g is grand-staircase learnable if $E_{gst}^* = \mathbb{R}^p$.

Using proposition 5.1 and certain simplifying properties of the Bayes-AMP dynamics, we can show (see S.I.) that for large enough α , AMP recovers E_{gst}^* :

Theorem 5.2. For any δ , there exists $\alpha > \alpha_c$ such that with arbitrarily small side-information $\sqrt{\lambda}$, with high probability as $d \rightarrow \infty$, $\mathbf{M}_d^t \succ \delta M_{E_{gst}^*}$ in $t = \mathcal{O}(\log^{1/\lambda})$ iterations, where $M_{E_{gst}^*} \in \mathcal{S}_p^+$ spans E_{gst}^* .

Final remarks — We stress that grand staircase functions are *not* equivalent to the staircase ones of (Abbe et al., 2022; 2023). Consider for instance

$$g(\mathbf{z}) = \text{He}_4(z_1) + \text{sign}(z_1 z_2 z_3). \quad (27)$$

As for (24), it can be AMP-learned with $\mathcal{O}(d)$ samples by first recovering the direction corresponding to z_1 . Unlike (24), however, which is “leap 2” under the CSQ staircase classification, $g(\mathbf{z})$ is “leap 3”. The CSQ lower-bound therefore implies a sample complexity-requirement of $\Omega(d^{1.5})$ with online-SGD learning it in $\mathcal{O}(d^2)$ samples.

We expect *grand staircase functions* to be efficiently learnable by two-layers nets if data reusing is allowed (while only *standard staircase* ones are learned with single-pass SGD). Arnaboldi et al. (2024) recently provided strong evidence that they can indeed be learned in $\mathcal{O}(d \log d)$ steps. The analysis of Joshi et al. (2024) is compatible with this conjecture. We hope our study will spark more work in this direction.

Acknowledgements

The authors would like to thank Joan Bruna, Theodor Misiakiewicz, Luca Pesce, and Nati Srebro for stimulating discussions. This work was supported by the Swiss National Science Foundation under grants SNSF SMArtNet (grant number 212049) and SNSF OperaGOST (grant number 200390) and the Choose France - CNRS AI Rising Talents program.

References

Emmanuel Abbe, Enric Boix Adsera, and Theodor Misiakiewicz. The merged-staircase property: a necessary and nearly sufficient condition for sgd learning of sparse functions on two-layer neural networks. In Po-Ling Loh and Maxim Raginsky, editors, *Proceedings of Thirty Fifth Conference on Learning Theory*, volume 178 of *Proceedings of Machine Learning Research*, pages 4782–4887. PMLR, 02–05 Jul 2022. URL <https://proceedings.mlr.press/v178/abbe22a.html>.

Emmanuel Abbe, Enric Boix Adserà, and Theodor Misiakiewicz. Sgd learning on neural networks: leap complexity and saddle-to-saddle dynamics. In Gergely Neu and Lorenzo Rosasco, editors, *Proceedings of Thirty Sixth Conference on Learning Theory*, volume 195 of *Proceedings of Machine Learning Research*, pages 2552–2623. PMLR, 12–15 Jul 2023. URL <https://proceedings.mlr.press/v195/abbe23a.html>.

Luca Arnaboldi, Ludovic Stephan, Florent Krzakala, and Bruno Loureiro. From high-dimensional & mean-field dynamics to dimensionless odes: A unifying approach to sgd in two-layers networks. In Gergely Neu and Lorenzo Rosasco, editors, *Proceedings of Thirty Sixth Conference on Learning Theory*, volume 195 of *Proceedings of Machine Learning Research*, pages 1199–1227. PMLR, 12–15 Jul 2023. URL <https://proceedings.mlr.press/v195/arnaboldi23a.html>.

Luca Arnaboldi, Yatin Dandi, Florent Krzakala, Luca Pesce, and Ludovic Stephan. Repetita iuvant: Data repetition allows sgd to learn high-dimensional multi-index functions. *arXiv preprint arXiv:2405.15459*, 2024.

Gerard Ben Arous, Reza Gheissari, and Aukosh Jagannath. Online stochastic gradient descent on non-convex losses from high-dimensional inference. *Journal of Machine Learning Research*, 22(106):1–51, 2021. URL <http://jmlr.org/papers/v22/20-1288.html>.

Benjamin Aubin, Antoine Maillard, Jean Barbier, Florent Krzakala, Nicolas Macris, and Lenka Zdeborová. The committee machine: computational to statistical gaps in learning a two-layers neural network*. *Journal of Statistical Mechanics: Theory and Experiment*, 2019(12):124023, dec 2019. doi: 10.1088/1742-5468/ab43d2. URL <https://dx.doi.org/10.1088/1742-5468/ab43d2>.

Benjamin Aubin, Florent Krzakala, Yue Lu, and Lenka Zdeborová. Generalization error in high-dimensional perceptrons: Approaching bayes error with convex optimization. In H. Larochelle, M. Ranzato, R. Hadsell, M.F. Balcan, and H. Lin, editors, *Advances in Neural Information Processing Systems*, volume 33, pages 12199–12210. Curran Associates, Inc., 2020a. URL https://proceedings.neurips.cc/paper_files/paper/2020/file/8f4576ad85410442a74ee3a7683757b3-Paper.pdf.

Benjamin Aubin, Bruno Loureiro, Antoine Baker, Florent Krzakala, and Lenka Zdeborová. Exact asymptotics for phase retrieval and compressed sensing with random generative priors. In Jianfeng Lu and Rachel Ward, editors, *Proceedings of The First Mathematical and Scientific Machine Learning Conference*, volume 107 of *Proceedings of Machine Learning Research*, pages 55–73. PMLR, 20–24 Jul 2020b. URL <https://proceedings.mlr.press/v107/aubin20a.html>.

Jimmy Ba, Murat A Erdogdu, Taiji Suzuki, Zhichao Wang, Denny Wu, and Greg Yang. High-dimensional asymptotics of feature learning: How one gradient step improves the representation. In S. Koyejo, S. Mohamed, A. Agarwal, D. Belgrave, K. Cho, and A. Oh, editors, *Advances in Neural Information Processing Systems*, volume 35, pages 37932–37946. Curran Associates, Inc., 2022. URL https://proceedings.neurips.cc/paper_files/paper/2022/file/f7e7fabd73b3df96c54a320862afcb78-Paper-Conference.pdf.

Dmitry Babichev and Francis Bach. Slice inverse regression with score functions. *Electronic Journal of Statistics*, 12(1):1507 – 1543, 2018. doi: 10.1214/18-EJS1428. URL <https://doi.org/10.1214/18-EJS1428>.

Afonso S Bandeira, Amelia Perry, and Alexander S Wein. Notes on computational-to-statistical gaps: predictions using statistical physics. *Portugaliae mathematica*, 75(2):159–186, 2018.

Afonso S Bandeira, Ahmed El Alaoui, Samuel Hopkins, Tselil Schramm, Alexander S Wein, and Ilias Zadik. The franz-parisi criterion and computational trade-offs in high dimensional statistics. In S. Koyejo, S. Mohamed, A. Agarwal, D. Belgrave, K. Cho, and A. Oh, editors, *Advances in Neural Information Processing Systems*, volume 35, pages 33831–33844. Curran Associates, Inc., 2022. URL https://proceedings.neurips.cc/paper_files/paper/2022/file/daff682411a64632e083b9d6665b1d30-Paper-Conference.pdf.

Jean Barbier, Florent Krzakala, Nicolas Macris, Léo Miolane, and Lenka Zdeborová. Optimal errors and phase transitions in high-dimensional generalized linear models. *Proceedings of the National Academy of Sciences*, 116(12):5451–5460, 2019. doi: 10.1073/pnas.1802705116. URL <https://www.pnas.org/doi/abs/10.1073/pnas.1802705116>.

Mohsen Bayati and Andrea Montanari. The dynamics of message passing on dense graphs, with applications to compressed sensing. *IEEE Transactions on Information Theory*, 57(2):764–785, 2011. doi: 10.1109/TIT.2010.2094817.

Raphaël Berthier, Andrea Montanari, and Kangjie Zhou. Learning time-scales in two-layers neural networks. *arXiv preprint arXiv:2303.00055*, 2023.

Alberto Bietti, Joan Bruna, and Loucas Pillaud-Vivien. On learning gaussian multi-index models with gradient flow. *arXiv preprint arXiv:2310.19793*, 2023.

Avrim Blum, Merrick Furst, Jeffrey Jackson, Michael Kearns, Yishay Mansour, and Steven Rudich. Weakly learning dnf and characterizing statistical query learning using fourier analysis. *Proceedings of the Twenty-Sixth Annual Symposium on Theory of Computing*, 10 1994. doi: 10.1145/195058.195147.

Avrim Blum, Adam Kalai, and Hal Wasserman. Noise-tolerant learning, the parity problem, and the statistical query model. *J. ACM*, 50(4):506–519, jul 2003. ISSN 0004-5411. doi: 10.1145/792538.792543. URL <https://doi.org/10.1145/792538.792543>.

David R. Brillinger. *A Generalized Linear Model With “Gaussian” Regressor Variables*, pages 589–606. Springer New York, New York, NY, 1982. ISBN 978-1-4614-1344-8. doi: 10.1007/978-1-4614-1344-8_34. URL https://doi.org/10.1007/978-1-4614-1344-8_34.

Michael Celentano, Andrea Montanari, and Yuchen Wu. The estimation error of general first order methods. In Jacob Abernethy and Shivani Agarwal, editors, *Proceedings of Thirty Third Conference on Learning Theory*, volume 125 of *Proceedings of Machine Learning Research*, pages 1078–1141. PMLR, 09–12 Jul 2020. URL <https://proceedings.mlr.press/v125/celentano20a.html>.

Sitan Chen and Raghu Meka. Learning polynomials in few relevant dimensions. In Jacob Abernethy and Shivani Agarwal, editors, *Proceedings of Thirty Third Conference on Learning Theory*, volume 125 of *Proceedings of Machine Learning Research*, pages 1161–1227. PMLR, 09–12 Jul 2020. URL <https://proceedings.mlr.press/v125/chen20a.html>.

Sitan Chen, Aravind Gollakota, Adam Klivans, and Raghu Meka. Hardness of noise-free learning for two-hidden-layer neural networks. *Advances in Neural Information Processing Systems*, 35:10709–10724, 2022.

Elizabeth Collins-Woodfin, Courtney Paquette, Elliot Paquette, and Inbar Seroussi. Hitting the high-dimensional notes: An ode for sgd learning dynamics on glms and multi-index models. *arXiv preprint arXiv:2308.08977*, 2023.

Arnak S. Dalalyan, Anatoly Juditsky, and Vladimir Spokoiny. A new algorithm for estimating the effective dimension-reduction subspace. *Journal of Machine Learning Research*, 9(53):1647–1678, 2008. URL <http://jmlr.org/papers/v9/dalalyan08a.html>.

Alex Damian, Eshaan Nichani, Rong Ge, and Jason D Lee. Smoothing the landscape boosts the signal for sgd: Optimal sample complexity for learning single index models. In A. Oh, T. Naumann, A. Globerson, K. Saenko, M. Hardt, and S. Levine, editors, *Advances in Neural Information Processing Systems*, volume 36, pages 752–784. Curran Associates, Inc., 2023. URL https://proceedings.neurips.cc/paper_files/paper/2023/file/02763667a5761ff92bb15d8751bcd223-Paper-Conference.pdf.

Alex Damian, Lucas Pillaud-Vivien, Jason D. Lee, and Joan Bruna. Computational-statistical gaps in gaussian single-index models. *arXiv preprint arXiv:2403.05529*, 2024.

Alexandru Damian, Jason Lee, and Mahdi Soltanolkotabi. Neural networks can learn representations with gradient descent. In Po-Ling Loh and Maxim Raginsky, editors, *Proceedings of Thirty Fifth Conference on Learning Theory*, volume 178 of *Proceedings of Machine Learning Research*, pages 5413–5452. PMLR, 02–05 Jul 2022.

Yatin Dandi, Emanuele Troiani, Luca Arnaboldi, Luca Pesce, Lenka Zdeborová, and Florent Krzakala. The benefits of reusing batches for gradient descent in two-layer networks: Breaking the curse of information and leap exponents. *arXiv preprint arXiv:2402.03220*, 2024.

Aurelien Decelle, Florent Krzakala, Cristopher Moore, and Lenka Zdeborová. Inference and phase transitions in the detection of modules in sparse networks. *Physical Review Letters*, 107(6):065701, 2011.

Yash Deshpande and Andrea Montanari. Finding hidden cliques of size $\sqrt{N/e}$ in nearly linear time. *Foundations of Computational Mathematics*, 15:1069–1128, 2015.

Ilias Diakonikolas, Daniel M. Kane, Vasilis Kontonis, and Nikos Zarifis. Algorithms and sq lower bounds for pac learning one-hidden-layer relu networks. In Jacob Abernethy and Shivani Agarwal, editors, *Proceedings of Thirty Third Conference on Learning Theory*, volume 125 of *Proceedings of Machine Learning Research*, pages 1514–1539. PMLR, 09–12 Jul 2020. URL <https://proceedings.mlr.press/v125/diakonikolas20d.html>.

David L. Donoho, Arian Maleki, and Andrea Montanari. Message-passing algorithms for compressed sensing. *Proceedings of the National Academy of Sciences*, 106(45):18914–18919, 2009. doi: 10.1073/pnas.0909892106. URL <https://www.pnas.org/doi/abs/10.1073/pnas.0909892106>.

Yihong Du. *Order structure and topological methods in nonlinear partial differential equations: Vol. 1: Maximum principles and applications*, volume 2. World Scientific, 2006.

Massimo Fornasier, Karin Schnass, and Jan Vybiral. Learning functions of few arbitrary linear parameters in high dimensions. *Foundations of Computational Mathematics*, 12(2):229–262, Apr 2012. ISSN 1615-3383. doi: 10.1007/s10208-012-9115-y. URL <https://doi.org/10.1007/s10208-012-9115-y>.

Jerome H. Friedman and Werner Stuetzle. Projection pursuit regression. *Journal of the American Statistical Association*, 76(376):817–823, 1981. ISSN 01621459. URL <http://www.jstor.org/stable/2287576>.

J.H. Friedman and J.W. Tukey. A projection pursuit algorithm for exploratory data analysis. *IEEE Transactions on Computers*, C-23(9):881–890, 1974. doi: 10.1109/T-C.1974.224051.

Cédric Gerbelot and Raphaël Berthier. Graph-based approximate message passing iterations. *Information and Inference: A Journal of the IMA*, 12(4):2562–2628, 09 2023. ISSN 2049-8772. doi: 10.1093/imaiai/iaad020. URL <https://doi.org/10.1093/imaiai/iaad020>.

Surbhi Goel, Aravind Gollakota, Zhihan Jin, Sushrut Karmalkar, and Adam Klivans. Superpolynomial lower bounds for learning one-layer neural networks using gradient descent. In *International Conference on Machine Learning*, pages 3587–3596. PMLR, 2020.

Alice Guionnet, Justin Ko, Florent Krzakala, Pierre Mergny, and Lenka Zdeborová. Spectral phase transitions in non-linear wigner spiked models. *arXiv preprint arXiv:2310.14055*, 2023.

Adel Javanmard and Andrea Montanari. State evolution for general approximate message passing algorithms, with applications to spatial coupling. *Information and Inference: A Journal of the IMA*, 2(2):115–144, 2013.

Nirmit Joshi, Theodor Misiakiewicz, and Nathan Srebro. On the complexity of learning sparse functions with statistical and gradient queries. *arXiv preprint arXiv:2407.05622*, 2024.

Yoshiyuki Kabashima. Inference from correlated patterns: a unified theory for perceptron learning and linear vector channels. In *Journal of Physics: Conference Series*, volume 95, page 012001. IOP Publishing, 2008.

Sham M Kakade, Varun Kanade, Ohad Shamir, and Adam Kalai. Efficient learning of generalized linear and single index models with isotonic regression. In J. Shawe-Taylor, R. Zemel, P. Bartlett, F. Pereira, and K.Q. Weinberger, editors, *Advances in Neural Information Processing Systems*, volume 24. Curran Associates, Inc., 2011. URL https://proceedings.neurips.cc/paper_files/paper/2011/file/30bb3825e8f631cc6075c0f87bb4978c-Paper.pdf.

Adam Tauman Kalai and Ravi Sastry. The isotron algorithm: High-dimensional isotonic regression. In *COLT 2009 - The 22nd Conference on Learning Theory, Montreal, Quebec, Canada, June 18-21, 2009*, 2009. URL <http://www.cs.mcgill.ca/%7Ecolt2009/papers/001.pdf#page=1>.

Michael Kearns. Efficient noise-tolerant learning from statistical queries. *J. ACM*, 45(6):983–1006, nov 1998. ISSN 0004-5411. doi: 10.1145/293347.293351. URL <https://doi.org/10.1145/293347.293351>.

Mark Grigor'evich Krein and Moisei Aronovich Rutman. Linear operators leaving invariant a cone in a banach space. *Uspekhi Matematicheskikh Nauk*, 3(1):3–95, 1948.

Florent Krzakala, Cristopher Moore, Elchanan Mossel, Joe Neeman, Allan Sly, Lenka Zdeborová, and Pan Zhang. Spectral redemption in clustering sparse networks. *Proceedings of the National Academy of Sciences*, 110(52):20935–20940, 2013.

Jason D Lee, Kazusato Oko, Taiji Suzuki, and Denny Wu. Neural network learns low-dimensional polynomials with sgd near the information-theoretic limit. *arXiv preprint arXiv:2406.01581*, 2024.

Gen Li and Yuting Wei. A non-asymptotic framework for approximate message passing in spiked models. *arXiv preprint arXiv:2208.03313*, 2022.

Gen Li, Wei Fan, and Yuting Wei. Approximate message passing from random initialization with applications to $z=2$ synchronization. *Proceedings of the National Academy of Sciences*, 120(31):e2302930120, 2023.

Ker-Chau Li. Sliced inverse regression for dimension reduction. *Journal of the American Statistical Association*, 86(414):316–327, 1991. ISSN 01621459. URL <http://www.jstor.org/stable/2290563>.

Yue M Lu and Gen Li. Phase transitions of spectral initialization for high-dimensional non-convex estimation. *Information and Inference: A Journal of the IMA*, 9(3):507–541, 2020.

Wangyu Luo, Wael Alghamdi, and Yue M Lu. Optimal spectral initialization for signal recovery with applications to phase retrieval. *IEEE Transactions on Signal Processing*, 67(9):2347–2356, 2019.

Antoine Maillard, Bruno Loureiro, Florent Krzakala, and Lenka Zdeborová. Phase retrieval in high dimensions: Statistical and computational phase transitions. In H. Larochelle, M. Ranzato, R. Hadsell, M.F. Balcan, and H. Lin, editors, *Advances in Neural Information Processing Systems*, volume 33, pages 11071–11082. Curran Associates, Inc., 2020. URL https://proceedings.neurips.cc/paper_files/paper/2020/file/7ec0dbe445813422897e04ad8424a5e-Paper.pdf.

Antoine Maillard, Florent Krzakala, Yue M Lu, and Lenka Zdeborová. Construction of optimal spectral methods in phase retrieval. In *Mathematical and Scientific Machine Learning*, pages 693–720. PMLR, 2022.

Marc Mézard. The space of interactions in neural networks: Gardner’s computation with the cavity method. *Journal of Physics A: Mathematical and General*, 22(12):2181, 1989.

Marco Mondelli and Andrea Montanari. Fundamental limits of weak recovery with applications to phase retrieval. *Foundations of Computational Mathematics*, 19(3):703–773, Jun 2019. ISSN 1615-3383. doi: 10.1007/s10208-018-9395-y. URL <https://doi.org/10.1007/s10208-018-9395-y>.

Marco Mondelli and Ramji Venkataraman. Approximate message passing with spectral initialization for generalized linear models. In *International Conference on Artificial Intelligence and Statistics*, pages 397–405. PMLR, 2021.

Behrad Moniri, Donghwan Lee, Hamed Hassani, and Edgar Dobriban. A theory of non-linear feature learning with one gradient step in two-layer neural networks. *arXiv preprint arXiv:2310.07891*, 2023.

Andrea Montanari and Yuchen Wu. Statistically optimal first order algorithms: A proof via orthogonalization. *arXiv preprint arXiv:2201.05101*, 2022.

Sundeept Rangan. Generalized approximate message passing for estimation with random linear mixing. In *2011 IEEE International Symposium on Information Theory Proceedings*, pages 2168–2172. IEEE, 2011.

Cynthia Rush and Ramji Venkataraman. Finite sample analysis of approximate message passing algorithms. *IEEE Transactions on Information Theory*, 64(11):7264–7286, 2018.

David Saad and Sara Solla. Dynamics of on-line gradient descent learning for multilayer neural networks. In D. Touretzky, M. C. Mozer, and M. Hasselmo, editors, *Advances in Neural Information Processing Systems*, volume 8. MIT Press, 1996.

David Saad and Sara A Solla. On-line learning in soft committee machines. *Physical Review E*, 52(4):4225, 1995.

Rodrigo Veiga, Ludovic Stephan, Bruno Loureiro, Florent Krzakala, and Lenka Zdeborová. Phase diagram of stochastic gradient descent in high-dimensional two-layer neural networks. In S. Koyejo, S. Mohamed, A. Agarwal, D. Belgrave, K. Cho, and A. Oh, editors, *Advances in Neural Information Processing Systems*, volume 35, pages 23244–23255. Curran Associates, Inc., 2022. URL https://proceedings.neurips.cc/paper_files/paper/2022/file/939bb847ebfd14c6e4d3b5705e562054-Paper-Conference.pdf.

Ming Yuan. On the identifiability of additive index models. *Statistica Sinica*, 21(4):1901–1911, 2011. ISSN 10170405, 19968507.

Lenka Zdeborová and Florent Krzakala. Statistical physics of inference: Thresholds and algorithms. *Advances in Physics*, 65(5):453–552, 2016.

Supplemental material

A Bayes optimality of AMP

We present in Alg.1 a detailed version of the AMP algorithm described in the text using the explicit notation of [Aubin et al. \(2019\)](#). While it was derived by [Aubin et al. \(2019\)](#) as a limit of Belief-Propagation, it can also be directly inferred from a multi-dimensional version of the standard AMP/GAMP for linear models [Rangan \(2011\)](#); [Javanmard and Montanari \(2013\)](#); [Zdeborová and Krzakala \(2016\)](#). As mentioned in the main, AMP Algorithm 1 is tailored to sample by estimating the posterior marginals Equation (7). AMP estimates the mean ω and variance \mathbb{V} of $\mathbf{W}^* \mathbf{x}$ and the mean $\widehat{\mathbf{W}}$ and covariance $\widehat{\mathbf{C}}$ of \mathbf{W}^* through a fixed point iteration. Note that the Onsager terms \mathbf{V}_i and \mathbf{A}_k can be made independent of the matrix by noting that the sum concentrate on the average of $\widehat{\mathbf{C}}$ and ∂g respectively.

Algorithm 1 Multi-index AMP

Input: Data $\mathbf{X} \in \mathbb{R}^{n \times d}$, $\mathbf{y} \in \mathbb{R}^n$
 Initialize $\hat{\mathbf{W}}^{t=0} \in \mathbb{R}^{p \times d}$, $\hat{\mathbf{C}}_k^{t=0} \in \mathcal{S}_p^+$ for $k \in [d]$, $\mathbf{g}^{t=0} \in \mathbb{R}^{n \times p}$.
for $t \leq T$ **do**
 /* Update likelihood mean and variance
 $\mathbf{V}_i^t = \sum_{k=1}^d X_{ik}^2 \hat{\mathbf{C}}_k^t \in \mathbb{R}^{p \times p}$; $\omega_i^t = \sum_{k=1}^d X_{ik} \hat{\mathbf{W}}_k^t - \mathbf{V}_i^t \mathbf{g}_i^{t-1} \in \mathbb{R}^p$, $i \in [n]$;
 $\mathbf{g}_i^t = \mathbf{g}_{\text{out}}(y_i, \omega_i^t, \mathbf{V}_i^t) \in \mathbb{R}^p$; $\partial \mathbf{g}_i^t = \partial \omega \mathbf{g}_{\text{out}}(y_i, \omega_i^t, \mathbf{V}_i^t) \in \mathbb{R}^{p \times p}$; $i \in [n]$
 /* Update prior first and second moments
 $\mathbf{A}_k^t = - \sum_{i=1}^n X_{ik}^2 \partial \mathbf{g}_i^t \in \mathbb{R}^{p \times p}$; $\mathbf{b}_k^t = \sum_{i \in [n]} X_{ik} \mathbf{g}_i^t + \mathbf{A}_k^t \hat{\mathbf{W}}_k^t$; $k \in [d]$
 $\hat{\mathbf{W}}_k^{t+1} = (\mathbf{I}_p + \mathbf{A}_k^t)^{-1} \mathbf{b}_k^t \in \mathbb{R}^p$; $\hat{\mathbf{C}}_k^{t+1} = (\mathbf{I}_p + \mathbf{A}_k^t)^{-1} \in \mathbb{R}^{p \times p}$, $k \in [d]$
end for
Return: Estimators $\hat{\mathbf{W}}_{\text{amp}} \in \mathbb{R}^{p \times d}$, $\hat{\mathbf{C}}_{\text{amp}} \in \mathbb{R}^{d \times p \times p}$

Sampling is, a priori, computationally prohibitive in the high-dimensional limit of interest here. The first impressive feat of AMP, a simple iterative first-order algorithm, is thus its efficiency. The second remarkable property of AMP is that its optimality with respect to the Bayesian posterior Equation (7) can be exactly characterised in the high-dimensional regime. Indeed, [Aubin et al. \(2019\)](#)—generalizing the earlier results of [Barbier et al. \(2019\)](#) on single index models—proved the following (formally, their proof was for the committee machine, but it applies *mutatis mutandis* to any multi-index models):

Theorem A.1 (Bayes-optimal correlation, Theorem 3.1 in [Aubin et al. \(2019\)](#), informal). *Let $(x_i, y_i)_{i \in [n]}$ denote n i.i.d. samples from the multi-index model defined in 1. Denote by $\hat{\mathbf{W}}_{\text{bo}} = \mathbb{E}[\mathbf{W}|X, y] \in \mathbb{R}^{p \times d}$ the mean of the posterior marginals Equation (7). Then, under Assumption 1 in the high-dimensional asymptotic limit where $n, d \rightarrow \infty$ with fixed ratio $\alpha = n/d$, the asymptotic correlation between the posterior mean and \mathbf{W}^* :*

$$\mathbf{M}^* = \lim_{d \rightarrow \infty} \mathbb{E} \left[\frac{1}{d} \hat{\mathbf{W}}_{\text{bo}} \mathbf{W}^{*\top} \right] \quad (28)$$

is the solution of the following supinf problem:

$$\sup_{\hat{\mathbf{M}} \in \mathcal{S}_p^+} \inf_{M \in \mathcal{S}_p^+} \left\{ -\frac{1}{2} \text{Tr } \mathbf{M} \hat{\mathbf{M}} - \frac{1}{2} \log \left(\mathbf{I}_p + \hat{\mathbf{M}} \right) + \frac{1}{2} \hat{\mathbf{M}} + \alpha H_Y(\mathbf{M}) \right\} \quad (29)$$

where $H_Y(\mathbf{M}) = \mathbb{E}_{\xi \sim \mathcal{N}(0, \mathbf{I}_p)}[H_Y(\mathbf{m}|\xi)]$, with $H_Y(\mathbf{M}|\xi)$ the the conditional entropy of the effective p -dimensional estimation problem Equation (10).

Note that the state evolution Equation (9) is closely related to the supinf problem in Equation (29). Indeed, remarking that the update function F in Equation (9) is precisely the gradient of the entropy H_Y in Equation (10), one can show that state evolution is equivalent to gradient descent in the objective defined by Equation (29) ([Aubin et al., 2019](#)). This non-trivial fact implies that whenever Equation (29) has a single

minima, AMP *optimally estimates* the posterior marginals, at least if its state evolution converges to this fixed point.

Finally, note that by construction $\hat{\mathbf{W}}_{\text{bo}}$ is the optimal estimator of \mathbf{W}^* given the data (X, y) (in the MMSE sense). Therefore, the rank of M^* defines the dimension of the statistically optimal subspace reconstruction at sample complexity $\alpha := n/a$. The fact that AMP follows state evolution is proven for such problems in (Javanmard and Montanari, 2013; Gerbelot and Berthier, 2023). Specifically, we refer to the example 4.4 in Gerbelot and Berthier (2023) on Matrix-valued random variables.

B Bayes-AMP in the presence of side-information

The algorithm is easily generalized to the case with *side information* of the type eq.(18):

$$\mathbf{S} = \sqrt{\lambda}W^* + \sqrt{1-\lambda}Z, \quad (30)$$

The effect of the additional side-information is equivalent to a modification of the prior on W to $P_W^S(W)$, defined as:

$$P_W^S(W) \propto P(\mathbf{S}|W)P_W(W) = \mathcal{N}(\sqrt{\lambda}\mathbf{S}, \sqrt{1-\lambda}\mathbf{I})$$

This is a simple consequence of Bayes theorem:

$$P(\mathbf{W}|\mathbf{y}, \mathbf{X}, \mathbf{S}) \propto P(\mathbf{y}, \mathbf{X}, \mathbf{S}|\mathbf{W})P_W(W) = P(\mathbf{y}, \mathbf{X}|\mathbf{W})P(\mathbf{S}|\mathbf{W})P_W(W) \quad (31)$$

In turns, this change updates of $\hat{\mathbf{W}}$ and $\hat{\mathbf{C}}$ in Algorithm 1 as described in Aubin et al. (2019):

$$\hat{\mathbf{W}}_k^{t+1} = (\mathbf{I}_p(1-\lambda) + \mathbf{A}_k^t)^{-1}(\mathbf{b}_k^t(1-\lambda) + \sqrt{\lambda}\mathbf{A}_k^t\mathbf{S}_k), \quad \hat{\mathbf{C}}_k^{t+1} = (\mathbf{I}_p(1-\lambda) + \mathbf{A}_k^t)^{-1}. \quad (32)$$

It is easily checked that the limit $\lambda \rightarrow 0$ gives back the equations in Algorithm 1. Lemma 2.1 is then modified with $G(X)$ in equation (9) being replaced by

$$G(X) = (X(1-\lambda) + \lambda)(1 + X(1-\lambda))^{-1}. \quad (33)$$

C Trivially-coupled Subspaces

In this section, we discuss and illustrate examples of g where $T_U^* \neq \emptyset$ for a learned subspace U . Our prototypical example throughout the discussion will be:

$$g(z_1, z_2, z_3) = z_1^2 + z_2^2 + \text{sign}(z_1 z_2 z_3). \quad (34)$$

Let e_1, e_2, e_3 denote the directions corresponding to components z_1, z_2, z_3 respectively. It is easy to check that for the above example, $E^* = \{e_1, e_2\}$ while $H_E^* = \{e_3\}$. Therefore, by Theorem 4.2, for large enough α the $\mathbf{M}^t \geq \delta M_E^*$ where M_E^* spans z_1, z_2 after $t = \mathcal{O}(\log \frac{1}{\lambda})$ iterations. Subsequently, since $T_{E^*}^* = \{e_3\}$, it gains an overlap along e_3 (independent of λ). Unlike sequential learning of directions in E_U^* , however, the time-steps for recovery of $\{e_1, e_2\}$ and $\{e_3\}$ (upto a threshold independent of λ) different only by a constant. The recovery of e_3 can therefore be interpreted as instantaneous w.r.t $\{e_1, e_2\}$.

D Proofs of the main results

In this section, we describe the proofs of our main results, starting with a *Trivial* proof of the learning of Trivial subspaces (Theorem 3.2) and the form of linearization that will be utilized throughout the analysis.

D.1 Theorem 3.2 and Linearization

Lemma 3.1 and Theorem 3.2 are direct consequences of the following observation:

Proposition D.1. *Let $\mathbf{v} \in \mathbb{R}^p$ be arbitrary. Then, starting from $\mathbf{M}^0 = 0$, $\mathbf{v}^\top \mathbf{M}^1 \mathbf{v} > 0$ if and only if:*

$$\alpha \mathbb{E} \left[\mathbf{v}^\top \mathbf{g}_{\text{out}}(Y^t, 0, \mathbf{I}_p) \mathbf{g}_{\text{out}}(Y^t, 0, \mathbf{I}_p)^\top \mathbf{v} \right] > 0 \quad (35)$$

Proof. The above proposition follows directly from the form of F in Lemma 2.1 and the observation that the mapping $G(X)$ preserves the span of X . \square

The expression in Equation 35 can be rewritten as:

$$\mathbb{E} [(\mathbf{v}^\top \mathbf{g}_{\text{out}}(Y^t, 0, \mathbf{I}_p))^2] \quad (36)$$

Since the operand inside the expectation is non-negative, the expectation is non-zero if and only if the operand vanishes identically. We therefore obtain Lemma 3.1 and Theorem 3.2.

D.1.1 Linearization without side-information

Our analysis relies on the following result:

Lemma D.2. *Let $F(\mathbf{M})$ be as defined in Lemma 2.1*

$$F(\mathbf{M}) \approx \alpha \mathcal{F}(\delta \mathbf{M}) + \mathcal{O}(\alpha \|\delta \mathbf{M}\|_F^2), \quad (37)$$

where $\|\cdot\|_F$ denotes the Frobenius norm and $\mathcal{F}(\delta \mathbf{M})$ is a linear operator on the cone \mathcal{S}_p^+ of PSD matrices of dimension p :

$$\mathcal{F}(\mathbf{M}) := \mathbb{E}_y [\partial_{\omega} \mathbf{g}_{\text{out}}(y, 0, \mathbf{I}_p) \mathbf{M} \partial_{\omega} \mathbf{g}_{\text{out}}(y, 0, \mathbf{I}_p)^\top], \quad (38)$$

We proceed through an-entry-wise expansion of each term inside the expectation in $F(\mathbf{M})$ around $\mathbf{M} = 0$. Recall that $\mathbf{g}_{\text{out}} \in \mathcal{C}^2$ by Assumption 1. Since $\mathbf{M}_F \leq p$, the first two derivatives of \mathbf{g}_{out} are uniformly bounded in \mathbf{g}_{out} for any fixed Y, ξ . Therefore, applying the multivariate Taylor expansion to $\mathbf{g}_{\text{out}}(Y^t, \Delta_1 \xi, I + \Delta_2)$, with $\Delta_1 = \sqrt{M}$ and $\Delta_2 = \mathbf{I}_p - \mathbf{M}$ yields:

$$\begin{aligned} & \mathbf{g}_{\text{out}}(Y^t, \sqrt{M^t} \xi, \mathbf{I}_p - \mathbf{M}^t) \mathbf{g}_{\text{out}}(Y^t, \sqrt{M^t} \xi, \mathbf{I}_p - \mathbf{M}^t)^\top \\ &= \mathbf{g}_{\text{out}}(Y^t, 0, \mathbf{I}_p - \mathbf{M}^t) \mathbf{g}_{\text{out}}(Y^t, 0, \mathbf{I}_p - \mathbf{M}^t)^\top + \partial_{\omega} \mathbf{g}_{\text{out}}(Y^t, 0, \mathbf{I}_p) \sqrt{M} \xi \xi^\top \sqrt{M}^\top \partial_{\omega} \mathbf{g}_{\text{out}}(Y^t, 0, \mathbf{I}_p)^\top \\ &+ \langle \partial_{\mathbf{V}} \mathbf{g}_{\text{out}}(Y^t, 0, \mathbf{I}_p) \mathbf{M} \rangle \mathbf{g}_{\text{out}}(Y^t, 0, \mathbf{I}_p)^\top + \mathbf{g}_{\text{out}}(Y^t, 0, \mathbf{I}_p) \langle \mathbf{M}, \partial_{\mathbf{V}} \mathbf{g}_{\text{out}}(Y^t, 0, \mathbf{I}_p) \rangle + \alpha C(\xi, y) \mathcal{O}(\|\mathbf{M}\|_F^2), \end{aligned}$$

where $C(\xi, Y)$ is an integrable function in ξ, Y . Since T^* is empty, $\mathbf{g}_{\text{out}}(Y^t, 0, \mathbf{I}_p)$ vanishes almost surely over y . Therefore, using dominated-convergence theorem, we obtain:

$$\begin{aligned} F(\mathbf{M}) &= \alpha \mathbb{E} \left[\mathbf{g}_{\text{out}}(Y^t, \sqrt{M^t} \xi, \mathbf{I}_p - \mathbf{M}^t) \mathbf{g}_{\text{out}}(Y^t, \sqrt{M^t} \xi, \mathbf{I}_p - \mathbf{M}^t)^\top \right] \\ &= \alpha \mathbb{E} \left[\partial_{\omega} \mathbf{g}_{\text{out}}(Y^t, 0, \mathbf{I}_p) \sqrt{M} \xi \xi^\top \sqrt{M}^\top \partial_{\omega} \mathbf{g}_{\text{out}}(Y^t, 0, \mathbf{I}_p)^\top \right] + \alpha \mathcal{O}(\|\mathbf{M}\|_F^2) \end{aligned}$$

Since at $\mathbf{M}^t = 0$, ξ and Y are independent, the above simplifies to:

$$F(\mathbf{M}) = \alpha \mathbb{E}_y [\partial_{\omega} \mathbf{g}_{\text{out}}(y, 0, \mathbf{I}_p - \mathbf{M}) \mathbf{M} \partial_{\omega} \mathbf{g}_{\text{out}}(y, 0, \mathbf{I}_p - \mathbf{M})^\top] + \alpha \mathcal{O}(\|\mathbf{M}\|_F^2)$$

D.1.2 Linearization in the presence of side-information

Analogous to Lemma D.2, we can linearize state-evolution in the presence of side-information in the limit of small M, λ .

Lemma D.3. Let $\mathcal{F}(\delta\mathbf{M})$ be a linear operator on the cone \mathcal{S}_p^+ of PSD matrices of dimension p , defined by:

$$\mathcal{F}(\mathbf{M}) := \mathbb{E}_y [\partial_{\omega} \mathbf{g}_{\text{out}}(y, 0, \mathbf{I}_p) \mathbf{M} \partial_{\omega} \mathbf{g}_{\text{out}}(y, 0, \mathbf{I}_p)^\top] \quad (39)$$

Then the following approximation holds:

$$F(\mathbf{M}) \approx \alpha \mathcal{F}(\delta\mathbf{M}) + \sqrt{\lambda} \mathbf{I}_d + \mathcal{O}(\alpha \|\delta\mathbf{M}\|_F^2) + \mathcal{O}(\lambda), \quad (40)$$

Proof. The above linearization is a direct consequence of Lemma D.2 along with the updated form of $G(X)$ in Equation 33. \square

D.2 Proof of Lemma 3.3

Proof. This is a direct consequence of the Tower law of expectation: $\mathbb{E} [\mathcal{T}(y) \langle \mathbf{v}^\top W^*, \mathbf{x} \rangle] = \mathbb{E}_y [\mathcal{T}(y) \mathbb{E}_{\mathbf{x}} [\langle \mathbf{v}^\top W^*, \mathbf{x} \rangle | y]]$

The statement then follows by noting that $\mathbf{g}_{\text{out}}(y, \mathbf{0}, \mathbf{I}_p)^\top \mathbf{v} = \lim_{d \rightarrow \infty} \mathbb{E}_{\mathbf{x}} [\langle \mathbf{v}^\top W^*, \mathbf{x} \rangle | y]$. The converse for any $v \in T^*$ then follows by setting $\mathcal{T}(y) = \mathbf{g}_{\text{out}}(y, \mathbf{0}, \mathbf{I}_p)$. \square

D.3 Proof of Lemma 4.1

Suppose that $M \in \mathcal{S}^+$, we have, for any $\mathbf{v} \in \mathbb{R}^p$:

$$\mathbf{v}^\top \mathcal{F}(\mathbf{M}) \mathbf{v} = \alpha \mathbb{E}_y [\mathbf{v}^\top \partial_{\omega} \mathbf{g}_{\text{out}}(y, 0, \mathbf{I}_p) \mathbf{M} \partial_{\omega} \mathbf{g}_{\text{out}}(y, 0, \mathbf{I}_p) \mathbf{v}], \quad (41)$$

since $\mathbf{M} \in \mathcal{S}^+$, each term inside the expectation is non-negative. Therefore:

$$\mathbf{v}^\top \mathcal{F}(\mathbf{M}) \mathbf{v} \geq 0 \quad (42)$$

Thus, $\mathcal{F}(M)$ is a cone-preserving linear map.

The generalised Perron-Frobenius theorem/Krein-Rutman Theorem for cone-preserving maps (Krein and Rutman, 1948; Du, 2006) then implies that the operator $\mathcal{F}(\mathbf{M})$ admits at-least one eigenvector $M^* \in \mathcal{S}_p^+$ corresponding to the largest eigenvalue $\nu_{\mathcal{F}}$ such that for any $M \in \mathcal{S}_p^+$:

$$\mathcal{F}(\mathbf{M}) \leq \nu_{\mathcal{F}} \|\mathbf{M}\|_F. \quad (43)$$

Furthermore, all other eigenvalues are strictly smaller than $\lambda_{\mathcal{F}}$. Subsequently, Lemma D.2 implies that $F(\mathbf{M})$ is stable at $\mathbf{M} = 0$ if and only if $\alpha \leq \frac{1}{\nu_{\mathcal{F}}} = \alpha_c$.

D.4 Proof of Theorem 4.2

Lemma 2.1 allows us to map the behavior of the variable \mathbf{M}^t in state-evolution to high-probability statements for the limiting overlaps.

Applying Lemmas D.3 and 3.3, we obtain that for small enough $\mathbf{M}^{t+1}, \lambda$:

$$\|\mathbf{M}^{t+1}\|_F \leq \alpha \nu_{\mathcal{F}} \|\mathbf{M}^t\|_F + \lambda + C_1 \|\mathbf{M}^t\|_F^2 + C_2 \|\mathbf{M}^t\|_F^2 \quad (44)$$

for some constants C_1, C_2 . Now, suppose that $\alpha < \frac{1}{\nu_{\mathcal{F}}}$. Then for $\|\mathbf{M}^t\|_F \geq \frac{1}{(1-\alpha\nu_{\mathcal{F}})} \lambda$, we have:

$$\alpha \nu_{\mathcal{F}} \|\mathbf{M}^t\|_F + \lambda \leq \|\mathbf{M}^t\|_F. \quad (45)$$

For small enough λ , we have that:

$$\mathbf{M}^0 \approx \lambda < \frac{1}{(1 - \alpha \nu_{\mathcal{F}})} \lambda. \quad (46)$$

Subsequently, by induction, we obtain that:

$$\sup_{t \geq p} \|\mathbf{M}^{t+1}\|_F \leq \frac{1}{(1 - \alpha \nu_{\mathcal{F}})} \lambda \quad (47)$$

for all $t > 0$. This proves the first part of the Theorem.

Now, suppose that $\alpha > \alpha_c$ or equivalently $\alpha\nu_F > 1$ and let $\mathbf{M}^* \in \mathcal{S}_p^+$ denote any of the eigenvectors of \mathcal{F} with eigenvalue ν_F , i.e. achieving the supremum in Equation 16.

From Lemma 4.1 and D.3, we obtain:

$$\text{tr}(\mathbf{M}^{t+1}, \mathbf{M}^*) \geq \alpha\nu_F \text{tr}(\mathbf{M}^t, \mathbf{M}^*) + \lambda - C_1 \|\mathbf{M}^t\|_F^2 - C_2 \lambda^2, \quad (48)$$

for some constants $C_1, C_2 > 0$.

Since $\alpha\nu_F > 1$, we obtain that $\text{tr}(\mathbf{M}^1, \mathbf{M}^*) > \lambda > 0$ for small enough λ .

Let $0 < \kappa < \nu_F - 1$ be fixed. Equation 48 implies that for $\frac{\text{tr}(\mathbf{M}^t, \mathbf{M}^*)}{\|\mathbf{M}^t\|_F^2} < \frac{\alpha\nu_F - 1 - \kappa}{C_1}$, and small enough λ :

$$\text{tr}(\mathbf{M}^{t+1}, \mathbf{M}^*) \geq (1 + \kappa) \text{tr}(\mathbf{M}^t, \mathbf{M}^*), \quad (49)$$

implying that $\text{tr}(\mathbf{M}^{t+1}, \mathbf{M}^*)$ grows as $\omega(e^{\kappa t})$. Since at $t = 1$, $\frac{\text{tr}(\mathbf{M}^t, \mathbf{M}^*)}{\|\mathbf{M}^t\|_F^2} = \mathcal{O}(\frac{1}{\lambda})$, Equation 44 implies that the condition $\frac{\text{tr}(\mathbf{M}^t, \mathbf{M}^*)}{\|\mathbf{M}^t\|_F^2} < \frac{\alpha\nu_F - 1 - \kappa}{C_1}$ holds for time $\mathcal{O}(\log \frac{1}{\lambda})$, which along with Equation 49 allows recovery upto an overlap δ independent of λ .

Finally, it remains to show that for large enough α , \mathbf{M}^t spans E^* .

Notice that for any $\mathbf{v} \in E^*$:

$$\mathbf{v}^\top \mathcal{F}(\mathbf{v}\mathbf{v}^\top) \mathbf{v} = \mathbb{E}_y [(\mathbf{v}^\top \partial_\omega \mathbf{g}_{\text{out}}(y, 0, \mathbf{I}_p) \mathbf{v})^2] > 0, \quad (50)$$

Define the smallest eigenvalue of \mathcal{F} :

$$\nu_{\mathcal{F}}^* = \inf_{\mathbf{v} \in E^*, \|\mathbf{v}\|=1} \mathbf{v}^\top \mathcal{F}(\mathbf{v}\mathbf{v}^\top) \mathbf{v}. \quad (51)$$

Since \mathbf{v} lies in a compact set, $\nu_{\mathcal{F}}^* > 0$.

Let $\mathbf{v}_1, \dots, \mathbf{v}_k$ denote an orthonormal basis for E^*

$$\mathbf{v}_i^\top (\mathbf{M}^{t+1}) \mathbf{v}_i \geq \alpha\nu_F \mathbf{v}_i^\top (\mathbf{M}^t) \mathbf{v}_i + \lambda - \alpha C \|\mathbf{M}^t\|_F^2. \quad (52)$$

Therefore, for $\alpha \geq \frac{1}{\nu_{\mathcal{F}}}$ and small enough ϵ , \mathbf{M}^t expands linearly along each \mathbf{v}_i .

D.5 Proof of Lemma 4.3

From the definition of \mathbf{g}_{out} in Equation 6 and the dominated-convergence theorem, it is straightforward to see that:

$$\partial_\omega \mathbf{g}_{\text{out}}(Y, \omega = \mathbf{0}, \mathbf{I}) = \mathbb{E}[\mathbf{Z}\mathbf{Z}^\top - \mathbf{I}|Y]. \quad (53)$$

Therefore for any $\mathbf{v} \in \mathbb{R}^p$ with $\|\mathbf{v}\| = 1$:

$$\begin{aligned} \mathbf{v}^\top \partial_\omega \mathbf{g}_{\text{out}}(Y, \omega, \mathbf{I})_{\omega=\mathbf{0}} \mathbf{v} &= \mathbb{E}[(\mathbf{v}^\top \mathbf{Z})^2 - 1|Y] \\ &= \lim_{d \rightarrow \infty} \mathbb{E}[\text{He}_2(\langle \mathbf{v}^\top \mathbf{W}^* \mathbf{x} \rangle) | \mathbf{y} = \mathbf{Y}], \end{aligned}$$

where the last expectation is w.r.t the joint measure $p(\mathbf{x}, y)$ defined in Definition 1.

Now, for any measurable transformation $\mathcal{T} : \mathbb{R} \rightarrow \mathbb{R}$, we have, by the tower law of expectation:

$$\mathbb{E} [\mathcal{T}(y) \text{He}_2(\langle \mathbf{v}^\top \mathbf{W}^* \mathbf{x} \rangle)] = \mathbb{E}_y [\mathcal{T}(y) \mathbb{E}_\mathbf{x} [\text{He}_2(\langle \mathbf{v}^\top \mathbf{W}^* \mathbf{x} \rangle) | \mathbf{y}]]. \quad (54)$$

For any $\mathbf{v} \in H_E^*$, the integrand vanishes asymptotically almost surely over y . Therefore, the dominated-convergence theorem implies that for $\mathbf{v} \in H_E^*$:

$$\lim_{d \rightarrow \infty} \mathbb{E} [\mathcal{T}(y) \text{He}_2(\langle \mathbf{v}^\top \mathbf{W}^* \mathbf{x} \rangle)] = 0. \quad (55)$$

D.6 Staircase Dynamics and the proof of Proposition 5.1

Before proving Proposition 5.1, we start by proving a monotonicity property of the AMP iterates, which in-turn implies that the AMP iterates gaining overlap along a certain subspace must eventually reach an approximate fixed point.

D.6.1 Monotonicity of the AMP Iterates

We begin by showing that the overlaps of the Bayes-AMP iterates is non-decreasing in the following sense:

Lemma D.4. *Consider the AMP algorithm with the Bayes-optimal choice of f_t, g_t . Then for any $t > 0$:*

$$\mathbf{M}^{(t+1)} \succeq \mathbf{M}^{(t)} \quad (56)$$

Proof. Our proof relies on a characterization of the state-evolution for the Bayes-AMP iterates as the solution to certain low-dimensional inference problems. See for instance [Barbier et al. \(2019\)](#); [Aubin et al. \(2019\)](#). Concretely, consider the following sequence of denoising problems over variables $Z^* \in \mathbb{R}^k, W^* \in \mathbb{R}^k$:

$$\begin{aligned} Y_t &= g(\sqrt{\mathbf{M}^{(t)}}\xi + \sqrt{\mathbb{I}_k - \mathbf{M}^{(t)}}Z^*) \\ \tilde{Y}_t &= \sqrt{\tilde{M}_t}W^* + Z \end{aligned}$$

where $Z, \xi \sim \mathcal{N}(0, \mathbf{I}_k)$ and \tilde{M}_t is obtained as:

$$\begin{aligned} \tilde{\mathbf{M}}^{(t)} &:= \mathbb{E} \left[(\mathbb{E}[Z^*|Y, \xi] \mathbb{E}[Z^*|Y, \xi]^\top) \right] \\ &= \mathbb{E} \left[g_{\text{out}}(Y, \sqrt{\mathbf{M}^{(t)}}\xi) g_{\text{out}}(Y, \sqrt{\mathbf{M}^{(t)}}\xi)^\top \right] \end{aligned} \quad (57)$$

We claim that the following statements hold for any $t > 0$:

$$\begin{aligned} \mathbf{M}^{(t+1)} &\succeq \mathbf{M}^{(t)} \\ \tilde{\mathbf{M}}^{(t+1)} &\succeq \tilde{\mathbf{M}}^{(t)} \end{aligned} \quad (58)$$

We proceed by induction. At $t = 0$, $\mathbf{M}^{(t)} = 0$ and thus $\mathbf{M}^{(t+1)} \succeq \mathbf{M}^{(t)}$ holds trivially. Subsequently, we show via an information-theoretic argument that $\mathbf{M}^{(t+1)} \succeq \mathbf{M}^{(t)}$ implies $\tilde{\mathbf{M}}^{(t+1)} \succeq \tilde{\mathbf{M}}^{(t)}$. Suppose that $\mathbf{M}^{(t+1)} \succeq \mathbf{M}^{(t)}$ holds at time-step t . We decompose the field entering the channel for Y_{t+1} as follows:

$$\begin{aligned} Y_{t+1} &= g(\sqrt{\mathbf{M}^{(t+1)}}\xi + \sqrt{\mathbb{I}_k - \mathbf{M}^{(t+1)}}Z^*) \\ &= g(\sqrt{\mathbf{M}^{(t)}}\xi_1 + \sqrt{\mathbf{M}^{(t+1)} - \mathbf{M}^{(t)}}\xi_2 + \sqrt{\mathbb{I}_k - \mathbf{M}^{(t+1)}}Z^*), \end{aligned}$$

where ξ_1, ξ_2 denote independent variables $\sim \mathcal{N}(0, 1)$. Now, compare the following two estimates:

$$\hat{Z}_1 = \mathbb{E}[Z^*|Y, \xi_1, \xi_2], \quad \hat{Z}_2 = \mathbb{E}[Z^*|Y, \xi_1]. \quad (59)$$

Note that by linearity of expectation and independence of ξ, Z^* , the estimator \hat{Z}_2 equals the estimator of the inference problem at time t :

$$Y_t = g(\sqrt{\mathbf{M}^{(t)}}\xi + \sqrt{\mathbb{I}_k - \mathbf{M}^{(t)}}Z^*) \quad (60)$$

By the optimality of the posterior-mean w.r.t MSE error, we must have for any $v \in \mathbb{R}^k$ with $\|v\| = 1$

$$\mathbb{E}[(\langle v, \hat{Z}_1 \rangle - \langle v, Z^* \rangle)^2] \leq \mathbb{E}[(\langle v, \hat{Z}_2 \rangle - \langle v, Z^* \rangle)^2] \quad (61)$$

, where $\langle v, \hat{Z}_i \rangle$ for $i = 1, 2$ denotes the projection of \hat{Z} along v or equivalently the Bayes-estimator of $\langle v, Z^* \rangle$. Now, a straightforward consequence of Bayes-rule (Nishimori's identity) implies that:

$$\mathbb{E}[\langle v, \hat{Z}_i \rangle \langle v, Z^* \rangle] = \mathbb{E}[(\langle v, \hat{Z}_i \rangle)^2], \quad (62)$$

for $i = 1, 2$. Substituting in Equation 61, we obtain:

$$\mathbb{E}[\langle v, \hat{Z}_1 \rangle \langle v, Z^* \rangle] \geq \mathbb{E}[\langle v, \hat{Z}_2 \rangle \langle v, Z^* \rangle]. \quad (63)$$

The above terms can be equivalently expressed as $v^\top \tilde{\mathbf{M}}^{(t+1)} v, v^\top \tilde{\mathbf{M}}^{(t)} v$ respectively. We obtain:

$$\tilde{\mathbf{M}}^{(t+1)} \succeq \tilde{\mathbf{M}}^{(t)}. \quad (64)$$

Similarly, we have that $\tilde{\mathbf{M}}^{(t+1)} \succeq \tilde{\mathbf{M}}^{(t)}$ implies $\mathbf{M}^{(t+2)} \succeq \mathbf{M}^{(t+1)}$. The claim therefore follows by induction. \square

D.6.2 Sequential visits to Fixed-points

Now, suppose that $E^* \neq \phi$ and consider the dynamics with side-information provided only along E^* i.e:

$$S = \sqrt{\lambda}P_{E^*} + \sqrt{1-\lambda}\mathbb{I}, + \quad (65)$$

where P_{E^*} denotes the projection along E^* . Suppose further tha $\alpha > \alpha_c$. By Theorem 4.2, $\mathbf{M}^{(t)} \succ \delta M_{E^*}$ in $\mathcal{O}(\log \frac{1}{\lambda})$ iterations. Since $G(X) \prec \mathbf{I}_k$ for any $X \in \mathcal{S}^+$, we have:

$$\mathbf{M}^{(t)} \prec \mathbf{I}_k, \quad (66)$$

for all $t > 0$. Considering the topology induced by the Frobenius norm on $\mathbb{R}^{p \times p}$, we obtain that $\mathbf{M}^{(t)}$ is a bounded sequence and therefore contains a convergent subsequence. By Lemma D.4, we obtain the the convergence of the entire sequence to a fixed point $\mathbf{M}_{E^*}^f(\lambda, \alpha)$.

Therefore, for any $\epsilon > 0$, $\exists t'$ such that for all $t > t'(\epsilon, \lambda)$:

$$\|\mathbf{M}^{(t)} - \mathbf{M}_{E^*}^f(\lambda, \alpha)\| \leq \epsilon. \quad (67)$$

Next, Lemma D.4 further implies that:

$$\mathbf{M}_{E^*}^f(\lambda, \alpha) \prec \mathbf{M}_{E^*}^f(\lambda', \alpha) \quad (68)$$

, for $\lambda < \lambda'$. Thus the following limit exists:

$$\mathbf{M}_{E^*}^f(\alpha) = \lim_{\lambda \rightarrow 0^+} \mathbf{M}_{E^*}^f(\lambda, \alpha). \quad (69)$$

We next show that for small enough λ , even with access to full side-information, the AMP iterates “visit” $\mathbf{M}_{E^*}^f$

Proposition D.5. *Suppose that $E^* \neq \phi$, $T^* = \phi$ and $T_{E^*}^* = \phi$, and $\alpha > \alpha_c$. Then under side-information $S = \sqrt{\lambda}W^* + \sqrt{1-\lambda}\mathbb{I}$, for any ϵ , for any $\epsilon > 0$ and small enough λ , there exists $t'(\epsilon, \lambda)$ such that for*

$$\|\mathbf{M}^{(t'(\epsilon, \lambda))} - \mathbf{M}_{E^*}^f(\alpha)\| \leq \epsilon. \quad (70)$$

Proof. Let $U = E^*$ and consider the linearized dynamics along the orthogonal complement $(U)_\perp$:

$$\mathcal{F}_{\mathbf{M}_U}(\mathbf{M}_\perp) := (\mathbf{I} + \mathbf{M}_U)^{-1} \mathbb{E}_y \left[\partial_{\boldsymbol{\omega}} \mathbf{g}_{\text{out}}(y, \sqrt{M_U} \boldsymbol{\xi}, \mathbf{I} - \sqrt{M_U}) \mathbf{M}_\perp \partial_{\boldsymbol{\omega}} \mathbf{g}_{\text{out}}(y, \sqrt{M_U} \boldsymbol{\xi}, \mathbf{I} - \sqrt{M_U})^\top \right], \quad (71)$$

where $\mathbf{M}_U \subseteq E^*$. By assumption, $\mathcal{F}_{\mathbf{M}_U}(\mathbf{M}_\perp) = 0$ for $\mathbf{M}_U = 0$. Therefore, by continuity of $\mathcal{F}_{\mathbf{M}_U}(\mathbf{M}_\perp)$ w.r.t \mathbf{M}_U , for any $\alpha > \alpha_c$, $\exists \delta > 0$ such that if $\mathbf{M}_U \prec \delta \mathbf{I}_p$, $\mathcal{F}_{\mathbf{M}_U}(\mathbf{M}_\perp)$ remains contractive. For small enough δ , we may therefore split the dynamics into two phases:

1. Phase 1: $0 < t < t_\delta$ where $t_\delta = \inf_{t>0} \mathbf{M}_U^t \succ \delta \mathbf{I}_p$.
2. Phase 2: $t > t_\delta$.

From Theorem 1, we know that $t_\delta = \mathcal{O}(\delta \log \frac{1}{\lambda})$. By the choice of δ , we have by the end of phase 1, $\mathbf{M}_\perp \prec C\lambda \mathbb{I}$ for some constant C_1 . By linearization D.3, we obtain that for t additional steps in Phase 2, the overlap along \mathbf{M}_\perp remains bounded by $e^{Kt\lambda}$ for some constant $K > 0$. We can further ensure that for small enough δ we can further ensure that $\mathbf{M}_U^{t_\delta} \prec C_2 \delta \mathbf{I}_p$, for some constant C_2 . Subsequently, by considering the limit $\delta \rightarrow 0$ with $\lambda \ll \delta$, and the roles of λ, δ interchanged, we obtain that after $\mathcal{O}(t'(\epsilon, \delta))$ additional steps, where $t'(\epsilon, \delta)$ is defined as in Equation 67:

$$\|\mathbf{M}^{(t'(\epsilon, \delta))} - \mathbf{M}_{E^*}^f(\alpha)\| \leq \epsilon \quad (72)$$

, since $t'(\epsilon, \delta)$ is independent of λ , the overlap along \mathbf{M}_\perp at $t'(\epsilon, \delta)$ remains $\mathcal{O}(\lambda)$. \square

The above proposition showed that, by restricting the side-information to specific subspaces, we can uniquely characterize sequences of fixed points along sequences of growing subspaces.

We're now ready to state the detailed version of Proposition 5.1 along with its proof, which states that upon the inclusion of additional side-information along a new subspace:

Proposition D.6 (Full-version of Proposition 5.1). *Let $U \subseteq \mathbb{R}^p$ be a subspace such that E_U^* is non-empty.. Consider AMP iterates with the Bayes-optimal choice of f_t, g_t with side-information restricted to the subspace U for sufficiently small $\lambda > 0$. Suppose that \mathbf{M}_U is a fixed-point under such a dynamics where \mathbf{M}_U spans U . Then, under the dynamics with an additional side-information along the subspace E_U^* :*

- For $\alpha > \alpha_{gst}(\mathbf{M}_U)$, AMP first reaches arbitrarily close to \mathbf{M}_U in $\mathcal{O}(\log \frac{1}{\lambda})$ iterations and subsequently recovers $M_{\mathbf{M}_U}^*$ in additional $\mathcal{O}(\log \frac{1}{\lambda})$ steps for arbitrarily small λ , where $M_{\mathbf{M}_U}^*$ denotes any matrix in \mathcal{S}_p^+ achieving the supremum $\sup_{\mathbf{M}^\perp \in U^\perp} \|\mathcal{F}_{\mathbf{M}_U}(\mathbf{M}^\perp)\|_F$ as per Definition (5).
- For $\alpha < \alpha_{gst}(\mathbf{M}_U)$ and sufficiently small λ , AMP reaches arbitrarily close to \mathbf{M}_U in $\mathcal{O}(\log \frac{1}{\lambda})$ and the overlap along E_U^* remains bounded by $C\lambda$.

Proof. By assumption, \mathbf{M}_U is a fixed point of $F(M)$ under the presence of side-information restricted to U . Therefore, Equation 9 implies that $\mathbf{g}_{\text{out}}(y, \boldsymbol{\omega}, \mathbf{I} - \sqrt{M_U})$ almost surely lies in U and thus T_U^* is empty. Therefore, by the proof of Proposition D.5, for sufficiently small λ , and any $\epsilon > 0$ AMP iterates reach ϵ -close to \mathbf{M}_U in time $\mathcal{O}(\log \frac{1}{\lambda})$ iterations, while the overlap along the orthogonal complement to \mathbf{M}_U being $\mathcal{O}(\lambda)$. Theorem 5.1 then follows that of 4.2 by considering the following linearized operator along U^\perp

$$\mathcal{F}_{\mathbf{M}_U}(\mathbf{M}_\perp) := (\mathbf{I} + \mathbf{M}_U)^{-1} \mathbb{E}_y \left[\partial_{\boldsymbol{\omega}} \mathbf{g}_{\text{out}}(y, \sqrt{M_U} \boldsymbol{\xi}, \mathbf{I} - \sqrt{M_U}) \mathbf{M}_\perp \partial_{\boldsymbol{\omega}} \mathbf{g}_{\text{out}}(y, \sqrt{M_U} \boldsymbol{\xi}, \mathbf{I} - \sqrt{M_U})^\top \right], \quad (73)$$

where $\boldsymbol{\omega} = \sqrt{M_U} \boldsymbol{\xi}$ with $\boldsymbol{\xi} \sim \mathcal{N}(0, \mathbf{I})$. Similar to Lemma D.2, the linearization follows by noting that y is independent of $\sqrt{M_\perp} \boldsymbol{\xi}$ and $\sqrt{M_U + M_\perp} = \sqrt{M_U} + \sqrt{M_\perp}$ since $\mathbf{M}_\perp \perp \mathbf{M}_U$. \square

D.7 Proof of Theorem 5.2

Theorem 5.2 follows by inductively applying Propositions 5.1 and D.5 as we describe below:

1. First, suppose that $T^* = \emptyset$ and $T_{E_k^*}^* = \emptyset$ for all $k \in \mathbb{N}$. By compactness, for any k , $\inf_{\mathbf{v} \in E_{E_k^*}^*} \mathbf{v}^\top \mathcal{F}_{\mathbf{M}_U}(\mathbf{M}_\perp) \mathbf{v} > 0$. Therefore, as in the proof of Theorem 1, for each E_k^* , $\exists \alpha_k$ such that for $\alpha > \alpha_k$, the corresponding fixed-point along E_k^* becomes unstable along the full subspace $E_{E_k^*}^*$, leading to weak-recovery of E_{k+1}^* in $\mathcal{O}(\log \frac{1}{\lambda})$ additional steps. Since k is bounded above by p , we obtain that $\alpha^* = \max_k \alpha_k$ is finite. For $\alpha > \alpha^*$, Proposition D.5 implies that AMP iterates sequentially visit E_k^* and eventually recover E_{gst}^* .
2. In the presence of trivial subspaces T^* , as shown in the proof of Theorem 3.2 and explained in section C, the trivially-coupled subspaces are learned instantaneously. Therefore, the sequence of fixed-points traversed by AMP span the following sequence of subspaces:

- (a) $U_1^* = T_1^{**}$.
- (b) $U_{j+1}^* = U_j^* \cup E_{U_j^*}^* \cup T_{E_{U_j^*}^*}^*$, for $j = 1, 2, \dots$,

where T_U^{**} denotes the maximal chain of trivial subspaces starting from U :

$$T_U^{**} = T_U^* \cup T_{T_U^*}^* \cup \dots \quad (74)$$

It is easy to check that the set subspaces $U \in \mathbb{R}^p$ is totally ordered under the span of $U \cup T_U^* \cup E_U^*$ and therefore possesses a unique maximal element. Therefore, both sequences U_i^* defined above and E_i^* defined in Definition 6 terminate at the same maximal element E_{gst}^* . Similar to (i), proposition D.5 then implies that for large enough α , and small enough λ AMP traverses the sequence of subspaces U_1^*, U_2^*, \dots , recovering E_{gst}^* in $\mathcal{O}(\log(\frac{1}{\lambda}))$ iterations.

E From AMP thresholds to Computational phase transitions for First-order algorithms

In this section, we discuss how Theorems 4.2 and 5.2 can be translated to rigorous lower-bounds on the sample complexity of weak-recovery from arbitrarily small initialization. For brevity, we omit the full-proof and provide a sketch of the argument based on existing results.

We recall the main results of (Celentano et al., 2020). (Celentano et al., 2020) consider the following class of general first-order algorithms (GFOM):

$$\mathbf{v}^t = \mathbf{X} f_t^{(1)}(\mathbf{u}^1, \dots, \mathbf{u}^t, \mathbf{y}, \mathbf{u}) + f_t^{(2)}(\mathbf{v}^1, \dots, \mathbf{v}^t, \mathbf{y}) \quad (75)$$

$$\mathbf{u}^{t+1} = \mathbf{X}^T g_t^{(1)}(\mathbf{v}^1, \dots, \mathbf{v}^t, \mathbf{v}) + g_t^{(2)}(\mathbf{u}^1, \dots, \mathbf{u}^t, \mathbf{y}, \mathbf{u}), \quad (76)$$

where $\mathbf{v}^t \in \mathbb{R}^{n \times r}$, $\mathbf{u}^t \in \mathbb{R}^{n \times r}$. Note that Algorithm 1 is a special case of the above class. The variables \mathbf{u}, \mathbf{v} encode additional side-information.

Subsequently, Celentano et al. (2020) show that any algorithm belonging to the above class can be mapped to a message-passing algorithm on an infinite-tree such that the errors of the GFOM algorithm at any finite-time t asymptotically match the errors of the surrogate estimation problem on the tree. For the tree-inference problem, the optimality of the Bayes-AMP directly follows from AMP being the dense-limit of the information-theoretically optimal Belief propagation on trees. This translates to the optimality of Bayes-optimal AMP at any finite-time t amongst GFOM algorithms.

Similar to our Theorem 1, Celentano et al. (2020) provide thresholds α_c for weak-recovery starting from arbitrarily small initialization in the case of sparse Phase retrieval and sparse PCA. As we discussed in Section B, the Bayes-optimal AMP in the presence of such side-information corresponds to a modified prior.

While Celentano et al. (2020) prove their results for the specific classes of high-dimensional regression (single-index) problems and low-rank matrix estimation, the underlying argument is general enough to be adapted to our setting of multi-index models. We therefore conjecture that the thresholds and class of problems described in Theorems 3.2, 1, 5.2 fundamentally characterize the learnability of multi-index models through first-order algorithms.

F Explicit results for some examples of the \mathbf{g}_{out} function

In this section, we list several problems, their corresponding \mathbf{g}_{out} , and analysis of their weak recoverability. For convenience we will use $\mathcal{Z}_{\text{out}}(y, \omega, \mathbf{V})$ defined as

$$\mathcal{Z}_{\text{out}}(y, \omega, \mathbf{V}) = \frac{1}{(2\pi)^{p/2}} \int_{\mathbb{R}^p} d\mathbf{z} e^{-\frac{1}{2}(\mathbf{z}-\omega)^\top \mathbf{V}^{-1}(\mathbf{z}-\omega)} P(y|\mathbf{z}) \quad (77)$$

which allows us to rewrite $\mathbf{g}_{\text{out}}(y, \omega, \mathbf{V})$

$$\mathbf{g}_{\text{out}}(y, \omega, \mathbf{V}) = \frac{1}{\mathcal{Z}_{\text{out}}(y, \omega, \mathbf{V})} \frac{1}{(2\pi)^{p/2}} \int_{\mathbb{R}^p} d\mathbf{z} e^{-\frac{1}{2}(\mathbf{z}-\omega)^\top \mathbf{V}^{-1}(\mathbf{z}-\omega)} P(y|\mathbf{z}) \mathbf{V}^{-1}(\mathbf{z}-\omega) \quad (78)$$

When computing the critical sample complexity we will also need $\partial_\omega \mathbf{g}_{\text{out}}(y, \omega, \mathbf{V})$, which can be expressed conveniently as

$$\begin{aligned} \partial_\omega \mathbf{g}_{\text{out}}(y, \omega, \mathbf{V}) &= \\ &\frac{1}{\mathcal{Z}_{\text{out}}(y, \omega, \mathbf{V})} \frac{1}{(2\pi)^{p/2}} \int_{\mathbb{R}^p} d\mathbf{z} e^{-\frac{1}{2}(\mathbf{z}-\omega)^\top \mathbf{V}^{-1}(\mathbf{z}-\omega)} (\mathbf{z}-\omega) P(y|\mathbf{z}) \mathbf{V}^{-2}(\mathbf{z}-\omega)^\top - \mathbf{V}^{-2} - \mathbf{g}_{\text{out}}(y, \omega, \mathbf{I}_p) \mathbf{g}_{\text{out}}(y, \omega, \mathbf{I}_p)^\top \end{aligned}$$

which becomes much simpler for $\mathbf{V} = \mathbf{I}_p$, $\omega = \mathbf{0}$, and $\mathbf{g}_{\text{out}}(y, \mathbf{0}, \mathbf{I}_p) = \mathbf{0}$:

$$\partial_\omega \mathbf{g}_{\text{out}}(y, \mathbf{0}, \mathbf{I}_p) = \frac{1}{\mathcal{Z}_{\text{out}}(y, \mathbf{0}, \mathbf{I}_p)} \frac{1}{(2\pi)^{p/2}} \int_{\mathbb{R}^p} d\mathbf{z} e^{-\frac{1}{2}\mathbf{z}^\top \mathbf{z}} (\mathbf{z}\mathbf{z}^\top - \mathbf{I}_p) P(y|\mathbf{z})$$

$$\mathbf{F.1} \quad g(z_1, z_2, \dots, z_p) = \prod_{j=1}^p z_j$$

In this subsection we will compute the critical sample complexity for this class of models. The first observation we can make is that for all p , $\mathbf{g}_{\text{out}}(y, \mathbf{0}, \mathbf{I}_p) = 0$. We can look at the cases $p = 2$ and $p \geq 3$ separately.

If $p = 2$ we have:

$$\mathcal{Z}_{\text{out}}(y, \mathbf{0}, \mathbf{I}_p) = \frac{K_0(|y|)}{\pi} \quad (79)$$

and

$$\partial_{\omega} \mathbf{g}_{\text{out}}(y, \mathbf{0}, \mathbf{I}_p) = \begin{bmatrix} y \frac{K_1(y)}{K_0(y)} - 1 & y \\ y & y \frac{K_1(y)}{K_0(y)} - 1 \end{bmatrix} \quad (80)$$

where $K_n(y)$ are the modified Bessel functions of the second kind. The integrals can be easily done in Mathematica. Since our model is invariant under permutations all the elements in the diagonal and out of diagonal need to take the same value.

If $p > 3$ the picture changes completely. First, we first have

$$\mathcal{Z}_{\text{out}}(y, \mathbf{0}, \mathbf{I}_p) = \frac{1}{(2\pi)^{p/2}} G_{0,p}^{p,0} \left(\frac{y^2}{2^p} \middle| \begin{array}{c} 0 \\ 0, 0, \dots, 0 \end{array} \right) \quad (81)$$

The next, crucial observation is that the out of diagonal terms of $\partial_{\mathbf{0}} \mathbf{g}_{\text{out}}(y, \mathbf{0}, \mathbf{I}_p)$ are zero. This is again a consequence of symmetry. We can see it in the practical example $p = 3$. From the explicit equation at the beginning of the appendix we see that out of diagonal elements of $\partial_{\mathbf{0}} \mathbf{g}_{\text{out}}(y, \mathbf{0}, \mathbf{I}_p)$ are proportional to the value of the following integral:

$$\frac{1}{(2\pi)^{3/2}} \int_{\mathbb{R}^3} dz e^{-\frac{z_1^2 + z_2^2 + z_3^2}{2}} z_1 z_2 \delta(y - z_1 z_2 z_3) \quad (82)$$

This integral is zero, as we can do a change of variable $\{z_1 \rightarrow z_1, z_2 \rightarrow -z_2, z_3 \rightarrow -z_3\}$: the delta function and the Gaussian measure are left unchanged, while $z_1 z_2$ switches sign. A similar approach can be used to show that out of diagonal elements are zero for every p .

The diagonal elements of $\partial_{\mathbf{0}} \mathbf{g}_{\text{out}}(y, \mathbf{0}, \mathbf{I}_p)$ take all the same value $f(y)$ because of permutation invariance of the argument of g , even though there is not a simple expression of them. We propose the following writing based on Meyer's G function

$$f(y) = 2G_{0,p}^{p,0} \left(\frac{y^2}{2^p} \middle| \begin{array}{c} 0 \\ 0, 0, \dots, 0, 1 \end{array} \right) / G_{0,p}^{p,0} \left(\frac{y^2}{2^p} \middle| \begin{array}{c} 0 \\ 0, 0, \dots, 0 \end{array} \right) - 1 \quad (83)$$

We are finally able to compute the critical sample complexity α_c . Unfortunately in the case $p = 2$ there is no immediate expression for α_c . Yet, it's possible to plug the expressions we just derived into (15) and perform the optimization in (16) numerically. The case $p \geq 3$ is much easier, as $\partial_{\mathbf{0}} \mathbf{g}_{\text{out}}(y, \mathbf{0}, \mathbf{I}_p) = f(y) \mathbf{I}_p$. We first start with (15)

$$\mathcal{F}(\mathbf{M}) = \mathbb{E}_Y [\partial_{\omega} \mathbf{g}_{\text{out}}(Y, \mathbf{0}, \mathbf{I}_p) \mathbf{M} \partial_{\omega} \mathbf{g}_{\text{out}}(Y, \mathbf{0}, \mathbf{I}_p)^{\top}] = \mathbb{E}_Y [f(Y)^2] M. \quad (84)$$

The alpha critical α_c will thus be

$$\alpha_c = \mathbb{E}_Y [f(Y)^2]^{-1} = \left[\int_{-\infty}^{\infty} dy f(y)^2 \mathcal{Z}_{\text{out}}(y) \right]^{-1} \quad (85)$$

Performing the integral numerically suggests the scaling law in the main text.

$$\mathbf{F.2} \quad \frac{1}{p} \sum_{i=1}^p z_i^2$$

We are only interested in computing the critical sample complexity for the case $p > 1$. The function g is even, so $\mathbf{g}_{\text{out}}(y, \mathbf{0}, \mathbf{I}_p) = 0$. The trick for the computation is to move to generalised spherical coordinates by choosing $r^2 = z_2^2 + \dots + z_p^2$. Recall that the area of the unit sphere in $p - 1$ dimensions is

$$\frac{2\pi^{\frac{p-1}{2}}}{\Gamma(\frac{p-1}{2})} \quad (86)$$

The matrix $\partial_{\omega} \mathbf{g}_{\text{out}}(y, \mathbf{0}, \mathbf{I}_p)$ is proportional to the identity. This is because we have permutation invariance with respect to the arguments in g , so the matrix $\partial_{\omega} \mathbf{g}_{\text{out}}(y, \mathbf{0}, \mathbf{I}_p)$ has the same value on the diagonal and the same off diagonal. The off diagonal elements are proportional to

$$\frac{1}{(2\pi)^{p/2}} \int_{\mathbb{R}^p} d\mathbf{z} e^{-\frac{1}{2} \sum_{i=1}^p z_i^2} z_1 z_2 \delta \left(y - \frac{1}{p} \sum_{i=1}^p z_i^2 \right) \quad (87)$$

If we do a change of variable $z_1 \rightarrow -z_1$ and all the other variables the same the integral changes sign, so this integral has to be zero. This shows that the matrix is diagonal, and because of the invariance under permutation also proportional to the identity. We are left to compute the actual value on the diagonal. First, we compute \mathcal{Z}_{out} :

$$\mathcal{Z}_{\text{out}}(y, \mathbf{0}, \mathbf{I}_p) = \frac{1}{(2\pi)^{p/2}} \int_{\mathbb{R}^p} d\mathbf{z} e^{-\frac{1}{2} \sum_{i=1}^p z_i^2} \delta \left(y - \frac{1}{p} \sum_{i=1}^p z_i^2 \right) \quad (88)$$

The integrand can be rewritten using the generalized spherical coordinates on the last $p-1$ variables

$$\frac{1}{(2\pi)^{p/2}} \int_{\mathbb{R}^p} d\mathbf{z} e^{-\frac{1}{2} \sum_{i=1}^p z_i^2} \delta \left(y - \frac{1}{p} \sum_{i=1}^p z_i^2 \right) = \frac{1}{2^{p/2-1} \Gamma \left(\frac{p-1}{2} \right) \sqrt{\pi}} \int_0^{+\infty} dr \int_{\mathbb{R}} dz_1 r^{p-2} e^{-\frac{z_1^2+r^2}{2}} \delta \left(y - \frac{z_1^2+r^2}{p} \right) \quad (89)$$

The last two integrals can be done by hand. Integrating over z_1 and then over r we get

$$\mathcal{Z}_{\text{out}}(y, \mathbf{0}, \mathbf{I}_p) = \frac{1}{2^{p/2-1} \Gamma \left(\frac{p-1}{2} \right) \sqrt{\pi}} \int_0^{\sqrt{py}} dr p r^{p-2} \frac{e^{-\frac{py}{2}}}{\sqrt{py-r^2}} = \frac{e^{-\frac{py}{2}}}{y^{2p/2} \Gamma \left(\frac{p}{2} \right)} (py)^{p/2} \quad (90)$$

One can proceed in the same fashion to show that

$$\frac{1}{(2\pi)^{p/2}} \int_{\mathbb{R}^p} d\mathbf{z} e^{-\frac{1}{2} \sum_{i=1}^p z_i^2} (z_1^2 - 1) \delta \left(y - \frac{1}{p} \sum_{i=1}^p z_i^2 \right) = \frac{e^{-\frac{py}{2}}}{y^{2p/2} \Gamma \left(\frac{p}{2} \right)} (py)^{p/2} (y-1), \quad (91)$$

which gives us the result

$$\partial_{\omega} \mathbf{g}_{\text{out}}(y, \mathbf{0}, \mathbf{I}_p) = (y-1) \mathbf{I}_p. \quad (92)$$

We can finally look at (15) and obtain

$$\mathcal{F}(\mathbf{M}) = \mathbb{E}_Y [(Y-1)^2] \mathbf{M} = \int_0^{+\infty} dy \frac{e^{-\frac{py}{2}}}{y^{2p/2} \Gamma \left(\frac{p}{2} \right)} (py)^{p/2} (y-1)^2 \mathbf{M} = \frac{2}{p} \mathbf{M} \quad (93)$$

from which it's immediate to obtain $\alpha_c = p/2$.

F.3 $g(z_1, \dots, z_p) = \text{sign}(\prod_{j=1}^p z_j)$

In this part of the section we will compute \mathbf{g}_{out} as in eq. (6) for arbitrary values of the argument. Define $\omega = (\omega_1, \dots, \omega_p)^\top$, $v_{ij} := (\mathbf{V}^{-1})_{i,j}$ and the Gaussian probability density

$$\rho(\mathbf{z} \in \mathbb{R}^p, \mathbf{V}) := \frac{1}{(2\pi)^{p/2} \sqrt{\det(\mathbf{V})}} e^{-\frac{1}{2} \mathbf{z}^\top \mathbf{V}^{-1} \mathbf{z}}. \quad (94)$$

Then, defining $\mathbb{R}_{+1} = [0, +\infty)$ and $\mathbb{R}_{-1} = (-\infty, 0]$, we have that eq. (77)

$$\mathcal{Z}_{\text{out}}(y, \omega, \mathbf{V}) = \int_{\mathbb{R}^p} dz_1 \dots dz_p \rho(\mathbf{z} - \omega, \mathbf{V}) \delta_{y, \text{sign}(z_1 \dots z_p)} \quad (95)$$

$$= \sum_{s_1, \dots, s_p = \pm 1} \delta_{y, (\prod_j s_j)} \int_{\mathbb{R}_{s_1}} dz_1 \dots \int_{\mathbb{R}_{s_p}} dz_p \rho(\mathbf{z} - \omega, \mathbf{V}). \quad (96)$$

In order to simplify this expression, we introduce the auxiliary function

$$\begin{aligned}
I_s(z_1, \dots, z_{p-1}, y, \boldsymbol{\omega}, \mathbf{V}) &:= \int_{\mathbb{R}_s} dz_p \frac{e^{-(\mathbf{z}-\boldsymbol{\omega})^T \mathbf{V}^{-1} (\mathbf{z}-\boldsymbol{\omega})}}{(2\pi)^{p/2} \sqrt{\det \mathbf{V}}} \\
&= \frac{e^{-\sum_{i,j=1}^{p-1} (z_i - \omega_i) v_{ij} (z_j - \omega_j)}}{(2\pi)^{p/2} \sqrt{\det \mathbf{V}}} \int_{\mathbb{R}_s} dz_p \exp \left(-v_{pp}(z_p - \omega_p)^2 - 2(z_p - \omega_p) \sum_{i=1}^{p-1} v_{ip}(z_i - \omega_i) \right) \\
&= \frac{e^{-\sum_{i,j=1}^{p-1} (z_i - \omega_i) (v_{ij} - v_{pp}^{-1} v_{ip} v_{jp}) (z_j - \omega_j)}}{2v_{pp} \sqrt{2} (2\pi)^{(p-1)/2} \sqrt{\det \mathbf{V}}} \left(1 - s \cdot \operatorname{erf} \left(\frac{\sum_{i=1}^{p-1} v_{ip}(z_i - \omega_i) - v_{pp}\omega_p}{\sqrt{v_{pp}}} \right) \right)
\end{aligned}$$

We introduce the matrix $\mathbf{d}(\mathbf{V}) \in \mathbb{R}^{(p-1) \times (p-1)}$ such that

$$d_{ij}(\mathbf{V}) := \det \begin{pmatrix} v_{ij} & v_{pi} \\ v_{jp} & v_{pp} \end{pmatrix}, \quad i, j \in 1, \dots, p-1, \quad (97)$$

and the function

$$E_s(\mathbf{z} \in \mathbb{R}^{p-1}, y, \boldsymbol{\omega}, \mathbf{V}) = \frac{1}{2\sqrt{2}v_{pp}} \left(1 - s \cdot \operatorname{erf} \left(\frac{\sum_{i=1}^{p-1} v_{ip}(z_i - \omega_i) - v_{pp}\omega_p}{\sqrt{v_{pp}}} \right) \right).$$

We can rewrite⁶

$$I_s(\mathbf{z} \in \mathbb{R}^{p-1}, y, \boldsymbol{\omega}, \mathbf{V}) := E_s(\mathbf{z}, y, \boldsymbol{\omega}, \mathbf{V}) \frac{\exp \left(-v_{pp}^{-1} \sum_{i,j=1}^{p-1} (z_i - \omega_i) d_{ij}(\mathbf{V}) (z_j - \omega_j) \right)}{(2\pi)^{(p-1)/2} \sqrt{\det(\mathbf{d}(\mathbf{V})^{-1})}} \quad (98)$$

$$= v_{pp}^{(p-1)/2} E_s(\mathbf{z}, y, \boldsymbol{\omega}, \mathbf{V}) \rho \left(\begin{pmatrix} z_1 - \omega_2 \\ \dots \\ z_{p-1} - \omega_{p-1} \end{pmatrix}, v_{pp} \mathbf{d}(\mathbf{V})^{-1} \right). \quad (99)$$

Therefore

$$\mathcal{Z}_{\text{out}}(y, \boldsymbol{\omega}, \mathbf{V}) = \sum_{s_1, \dots, s_p = \pm 1} \delta_{y, (\prod_j s_j)} \int_{\mathbb{R}_{s_1}} dz_1 \dots \int_{\mathbb{R}_{s_{p-1}}} dz_{p-1} I_{s_p}(\mathbf{z}, y, \boldsymbol{\omega}, \mathbf{V}) \quad (100)$$

$$= \sum_{s_1, \dots, s_{p-1} = \pm 1} \int_{\mathbb{R}_{s_1}} dz_1 \dots \int_{\mathbb{R}_{s_{p-1}}} dz_{p-1} I_{y s_1 \dots s_{p-1}}(\mathbf{z}, y, \boldsymbol{\omega}, \mathbf{V}). \quad (101)$$

The components of $\mathbf{g}_{\text{out}}(y, \boldsymbol{\omega}, \mathbf{V})$ are given by

$$\begin{aligned}
(\mathbf{g}_{\text{out}}(y, \boldsymbol{\omega}, \mathbf{V}))_p &= \frac{1}{\mathcal{Z}_{\text{out}}(y, \boldsymbol{\omega}, \mathbf{V})} \sum_{s_1, \dots, s_{p-1} = \pm 1} \int_{\mathbb{R}_{s_1}} dz_1 \dots \int_{\mathbb{R}_{s_{p-1}}} dz_{p-1} \frac{\partial}{\partial \omega_p} I_{y s_1 \dots s_{p-1}}(z_1, \dots, z_{p-1}, y, \boldsymbol{\omega}, \mathbf{V}) \\
&= \frac{1}{\mathcal{Z}_{\text{out}}(y, \boldsymbol{\omega}, \mathbf{V})} \sum_{s_1, \dots, s_{p-1} = \pm 1} y \prod_{j=1}^{p-1} s_j \int_{\mathbb{R}_{s_1}} dz_1 \dots \int_{\mathbb{R}_{s_{p-1}}} dz_{p-1} \rho \left(\begin{pmatrix} z_1 - \omega_1 \\ \dots \\ z_{p-1} - \omega_{p-1} \\ -\omega_p \end{pmatrix}, \mathbf{V} \right) \\
&= \frac{1}{\mathcal{Z}_{\text{out}}(y, \boldsymbol{\omega}, \mathbf{V})} \sum_{s_1, \dots, s_p = \pm 1} y \prod_{j \neq p} s_j \int_{\mathbb{R}_{s_1}} dz_1 \dots \int_{\mathbb{R}_{s_p}} dz_p \rho(\mathbf{z} - \boldsymbol{\omega}, \mathbf{V}) \delta(z_p),
\end{aligned}$$

and, analogously,

$$(\mathbf{g}_{\text{out}}(y, \boldsymbol{\omega}, \mathbf{V}))_k = \frac{1}{\mathcal{Z}_{\text{out}}(y, \boldsymbol{\omega}, \mathbf{V})} \sum_{s_1, \dots, s_p = \pm 1} y \prod_{j \neq k} s_j \int_{\mathbb{R}_{s_1}} dz_1 \dots \int_{\mathbb{R}_{s_p}} dz_p \rho(\mathbf{z} - \boldsymbol{\omega}, \mathbf{V}) \delta(z_k).$$

⁶It can be show that $\det(\mathbf{d}(\mathbf{V})) = \det(\mathbf{V}^{-1})$ by considering the defining properties of the determinant.

Stability of the fixed point and critical sample complexity We can now focus on studying the critical sample complexity. The first step is to compute $\partial_{\omega} \mathbf{g}_{\text{out}}(y, \mathbf{0}, \mathbf{I}_p)$ by using the identity

$$\partial_{\omega} \mathbf{g}_{\text{out}}(y, \mathbf{0}, \mathbf{I}) = \frac{1}{Z_{\text{out}}(y, \mathbf{0}, \mathbf{I})} \int d\mathbf{z} \frac{e^{-\frac{\mathbf{z}^\top \mathbf{z}}{2}}}{(2\pi)^{p/2}} (\mathbf{z} \mathbf{z}^\top - \mathbf{I}) \delta(y - g(\mathbf{z})) \quad (102)$$

To this end we know that

$$Z_{\text{out}}(y, \mathbf{0}, \mathbf{I}) = \frac{1}{(2\pi)^{p/2}} \int d\mathbf{z} e^{-\frac{\mathbf{z}^\top \mathbf{z}}{2}} \delta_{y, \text{sign}(z_1 \dots z_p)} = \frac{1}{2} \quad (103)$$

In order to compute $\partial_{\omega} \mathbf{g}_{\text{out}}(y, \mathbf{0}, \mathbf{I})$, we note at first that

$$\frac{1}{(2\pi)^{p/2}} \int d\mathbf{z} (z_k^2 - 1) e^{-\frac{\mathbf{z}^\top \mathbf{z}}{2}} \delta_{y, \text{sign}(z_1 \dots z_p)} = 0, \quad \forall k \in \{1, \dots, p\}. \quad (104)$$

For $p = 2$, consider the integral

$$\frac{1}{2\pi} \int dz_1 dz_2 z_1 z_2 e^{-\frac{z_1^2}{2} - \frac{z_2^2}{2}} \delta_{y, \text{sign}(z_1 \dots z_p)} \quad (105)$$

$$= \frac{2}{2\pi} \left(\delta_{y,1} \int_0^\infty dz_1 \int_0^\infty dz_2 z_1 z_2 e^{-\frac{z_1^2}{2} - \frac{z_2^2}{2}} + \delta_{y,-1} \int_0^\infty dz_1 \int_{-\infty}^0 dz_2 z_1 z_2 e^{-\frac{z_1^2}{2} - \frac{z_2^2}{2}} \right) \quad (106)$$

$$= \frac{\text{sign}(y)}{\pi} \quad (107)$$

Thus we have that

$$\partial_{\omega} \mathbf{g}_{\text{out}}(y, \mathbf{0}, \mathbf{I}) = \frac{2 \text{sign}(y)}{\pi} \begin{bmatrix} 0 & 1 \\ 1 & 0 \end{bmatrix} \quad (108)$$

Now we can notice that (16) simplifies significantly as $\partial_{\omega} \mathbf{g}_{\text{out}}(y, \mathbf{0}, \mathbf{I})$ is proportional to the counterdiagonal matrix for all values of y , thus having that

$$\mathcal{F}(\mathbf{M}) := \mathbb{E}_Y [\partial_{\omega} \mathbf{g}_{\text{out}}(Y, \mathbf{0}, \mathbf{I}_p) \mathbf{M} \partial_{\omega} \mathbf{g}_{\text{out}}(Y, \mathbf{0}, \mathbf{I}_p)^\top] = \frac{4}{\pi^2} \begin{bmatrix} 0 & 1 \\ 1 & 0 \end{bmatrix} \mathbf{M} \begin{bmatrix} 0 & 1 \\ 1 & 0 \end{bmatrix}$$

Finally we have that

$$\|\mathcal{F}(\mathbf{M})\|_F = \frac{4}{\pi^2} \left\| \begin{bmatrix} 0 & 1 \\ 1 & 0 \end{bmatrix} \mathbf{M} \begin{bmatrix} 0 & 1 \\ 1 & 0 \end{bmatrix} \right\|_F = \frac{4}{\pi^2} \|\mathbf{M}\|_F \quad (109)$$

Using (16) we obtain that α_c is simply

$\alpha_c = \pi^2/4$. For $p \geq 3$, defining $\mathbb{R}_{(\pm)}^p = \{\mathbf{z} \in \mathbb{R}^p \mid \text{sign}(z_1 \dots z_p) = \pm 1\}$, we need to compute integrals of the type

$$\begin{aligned} & \frac{1}{(2\pi)^{p/2}} \int_{\mathbb{R}_{(+)}^p} dz_1 \dots dz_p z_1 z_2 e^{-\frac{z_1^2}{2} \dots - \frac{z_p^2}{2}} \\ &= \frac{2}{2^{p-2} (2\pi)^{p/2}} \left(\sum_{j=0}^{\lfloor \frac{p-2}{2} \rfloor} \binom{p-2}{2j} \int_{\mathbb{R}_{(+)}^2} dz_1 dz_2 z_1 z_2 e^{-\frac{z_1^2}{2} - \frac{z_2^2}{2}} + \sum_{j=1}^{\lfloor \frac{p-1}{2} \rfloor} \binom{p-2}{2j-1} \int_{\mathbb{R}_{(-)}^2} dz_1 dz_2 z_1 z_2 e^{-\frac{z_1^2}{2} - \frac{z_2^2}{2}} \right) \\ &= \frac{2^{3-p}}{(2\pi)^{(p+2)/2}} \sum_{j=0}^{p-2} \binom{p-2}{j} (-1)^j = 0 \end{aligned}$$

In the same way it is possible to prove that the integral over $\mathbb{R}_{(-)}^p$ is also vanishing. This implies that $\partial_{\omega} \mathbf{g}_{\text{out}} = 0$, so using (16), we obtain that $\alpha_c = +\infty$. This model cannot be learned with $n = \mathcal{O}(d)$ samples for $p \geq 3$.

$$\mathbf{F.4} \quad g(z_1, \dots, z_p) = z_1^2 + \text{sign} \left(\prod_{j=1}^p z_j \right)$$

Following a procedure similar to Section F.3, we define $\boldsymbol{\omega} = (\omega_1, \dots, \omega_p)^\top$ and $v_{ij} := (\mathbf{V}^{-1})_{i,j}$.

We also introduce the matrix $\mathbf{d}(\mathbf{V}) \in \mathbb{R}^{(p-1) \times (p-1)}$ such that

$$d_{ij}(\mathbf{V}) := \det \begin{pmatrix} v_{i,j} & v_{i,p} \\ v_{j,p} & v_{p,p} \end{pmatrix}, \quad i, j \in 1, \dots, p, \quad (110)$$

the function

$$E_{s,s_1,s_p}(\mathbf{z} \in \mathbb{R}^{p-1}, y, \boldsymbol{\omega}, \mathbf{V}) = \frac{1}{2\sqrt{2}v_{pp}} \left(1 - s_p \cdot \text{erf} \left(\frac{v_{1p}(s_1\sqrt{y-s} - \omega_1) + \sum_{i=2}^{p-1} v_{ip}(z_i - \omega_i) - v_{pp}\omega_p}{\sqrt{v_{pp}}} \right) \right),$$

the Gaussian probability density

$$\rho(\mathbf{z} \in \mathbb{R}^p, \mathbf{V}) := \frac{1}{(2\pi)^{p/2} \sqrt{\det(\mathbf{V})}} e^{-\frac{1}{2}\mathbf{z}^\top \mathbf{V}^{-1} \mathbf{z}}, \quad (111)$$

and finally

$$I_{s,s_1,s_{p-1}}(\mathbf{z} \in \mathbb{R}^{p-1}, y, \boldsymbol{\omega}, \mathbf{V}) := \frac{E_{s,s_1,s_p}(\mathbf{z}, y, \boldsymbol{\omega}, \mathbf{V})}{2\sqrt{y-s}} \rho \left(\begin{pmatrix} s_1\sqrt{y-s} - \omega_1 \\ z_2 - \omega_2 \\ \dots \\ z_{p-1} - \omega_{p-1} \end{pmatrix}, v_{pp}\mathbf{d}(\mathbf{V})^{-1} \right).$$

Then, defining $\mathbb{R}_{+1} = [0, +\infty)$ and $\mathbb{R}_{-1} = (-\infty, 0]$, we have that

$$\mathcal{Z}_{\text{out}}(y, \boldsymbol{\omega}, \mathbf{V}) = \sum_{s, s_1, \dots, s_p = \pm 1} \delta_{s, (\prod_j s_j)} \mathbf{1}_{y > s} \int_{\mathbb{R}_{s_2}} dz_2 \dots \int_{\mathbb{R}_{s_{p-1}}} dz_{p-1} I_{s,s_1,s_p}(\mathbf{z}, y, \boldsymbol{\omega}, \mathbf{V}) \quad (112)$$

$$= \sum_{s, s_1, \dots, s_{p-1} = \pm 1} \mathbf{1}_{y > s} \int_{\mathbb{R}_{s_2}} dz_2 \dots \int_{\mathbb{R}_{s_{p-1}}} dz_{p-1} I_{s,s_1,s \cdot s_1 \dots s_{p-1}}(\mathbf{z}, y, \boldsymbol{\omega}, \mathbf{V}), \quad (113)$$

where $\mathbf{1}_{x>0}$ is the Heaviside step function. The components of $\mathbf{g}_{\text{out}}(y, \boldsymbol{\omega}, \mathbf{V})$ are given by

$$\begin{aligned} (\mathbf{g}_{\text{out}}(y, \boldsymbol{\omega}, \mathbf{V}))_1 &= \sum_{s, s_1, \dots, s_{p-1} = \pm 1} \frac{\mathbf{1}_{y > s}}{\mathcal{Z}_{\text{out}}(y, \boldsymbol{\omega}, \mathbf{V})} \int_{\mathbb{R}_{s_2}} dz_2 \dots \int_{\mathbb{R}_{s_{p-1}}} dz_{p-1} \frac{\partial}{\partial \omega_1} I_{s,s_1,s \cdot s_1 \dots s_{p-1}}(\mathbf{z}, y, \boldsymbol{\omega}, \mathbf{V}) \\ (\mathbf{g}_{\text{out}}(y, \boldsymbol{\omega}, \mathbf{V}))_{k \neq 1} &= \sum_{s, s_1, \dots, s_p = \pm 1} \frac{s \prod_{j \neq k} s_j \mathbf{1}_{y > s}}{\mathcal{Z}_{\text{out}}(y, \boldsymbol{\omega}, \mathbf{V})} \int_{\mathbb{R}_{s_2}} dz_2 \dots \int_{\mathbb{R}_{s_p}} dz_p \rho \left(\begin{pmatrix} s_1\sqrt{y-s} - \omega_1 \\ z_2 - \omega_2 \\ \dots \\ z_p - \omega_p \end{pmatrix}, \mathbf{V} \right) \delta(z_k) \end{aligned}$$

Stability of the fixed point We will use the same technique as F.3. The result is dependent on a number of integrals which we can compute analytically. First we have

$$\mathcal{Z}_{\text{out}}(y, \mathbf{0}, \mathbf{I}) = \frac{1}{(2\pi)^{p/2}} \int dz_1 \dots dz_p \delta(y - z_1^2 - \text{sign}(z_1 \dots z_p)) e^{-\frac{z_1^2}{2} - \dots - \frac{z_p^2}{2}} \quad (114)$$

$$= \frac{1}{2(2\pi)^{p/2}} \sum_{s_1, \dots, s_p = \pm 1} \frac{\mathbf{1}_{y > s}}{\sqrt{y - \prod_j s_j}} \int_{\mathbb{R}_{s_2}} dz_2 \dots \int_{\mathbb{R}_{s_{p-1}}} dz_{p-1} e^{-\frac{y-s_1 \dots s_p}{2} - \frac{z_2^2}{2} - \dots - \frac{z_p^2}{2}} \quad (115)$$

$$= \frac{1}{2\sqrt{2\pi}} \sum_{s=\pm 1} \mathbf{1}_{y > s} \frac{e^{-\frac{y-s}{2}}}{\sqrt{y-s}} \quad (116)$$

$$= \frac{e^{-y/2}}{2\sqrt{2\pi}e} \left(\frac{1}{\sqrt{y+1}} + \mathbf{1}_{y > 1} \frac{e}{\sqrt{y-1}} \right) \quad (117)$$

From this it is straightforward to see that $\mathbf{g}_{\text{out}}^0(y) = 0$. In order to compute $\nabla_{\omega}\mathbf{g}_{\text{out}}(y, 0, 1)$ we need to consider the additional integrals

$$1) \frac{1}{(2\pi)^{p/2}} \int dz_1 \dots dz_p (z_1^2 - 1) e^{-\frac{z_1^2}{2} - \dots - \frac{z_p^2}{2}} \delta(y - z_1^2 - \text{sign}(z_1 \dots z_p)) \quad (118)$$

$$= \frac{1}{2\sqrt{2\pi}} \sum_{s=\pm 1} \mathbf{1}_{y>s} \frac{e^{-\frac{y-s}{2}} (y-s-1)}{\sqrt{y-s}} \quad (119)$$

$$= \frac{e^{-y}}{2\sqrt{2\pi}e} \left(\frac{y}{\sqrt{y+1}} + \mathbf{1}_{y>1} \frac{e(y-2)}{\sqrt{y-1}} \right) \quad (120)$$

$$2) \frac{1}{(2\pi)^{p/2}} \int dz_1 \dots dz_p (z_{k\neq 1}^2 - 1) e^{-\frac{z_1^2}{2} - \dots - \frac{z_p^2}{2}} \delta(y - z_1^2 - \text{sign}(z_1 \dots z_p)) = 0 \quad (121)$$

$$3) \frac{1}{(2\pi)^{p/2}} \int dz_1 \dots dz_p z_j z_k e^{-\frac{z_1^2}{2} - \dots - \frac{z_p^2}{2}} \delta(y - z_1^2 - \text{sign}(z_1 \dots z_p)) \quad (122)$$

$$\propto \sum_{s, s_j, s_k = \pm 1} \mathbf{1}_{y>s} s_j s_k e^{-\frac{y-s}{2}} = 0 \quad (123)$$

$$(124)$$

This shows that

$$\mathcal{Z}_{\text{out}}(y, \mathbf{0}, \mathbf{I}_p) \partial_{\omega} \mathbf{g}_{\text{out}}(y, \mathbf{0}, \mathbf{I}_p) = \begin{bmatrix} C(y) & 0 & 0 \\ 0 & 0 & 0 \\ 0 & 0 & 0 \end{bmatrix} \quad (125)$$

where $C(y)$ is

$$C(y) = \begin{cases} y & -1 < y < 1 \\ y - 2e^{\frac{\sqrt{y+1}}{e\sqrt{y+1}+\sqrt{y-1}}} - 1 & y > 1 \end{cases} \quad (126)$$

This means that

$$\mathcal{F}(\mathbf{M}) := \mathbb{E}_Y [\partial_{\omega} \mathbf{g}_{\text{out}}(Y, \mathbf{0}, \mathbf{I}_p) \mathbf{M} \partial_{\omega} \mathbf{g}_{\text{out}}(Y, \mathbf{0}, \mathbf{I}_p)^{\top}] = \int dy C(y)^2 \mathcal{Z}_{\text{out}}(y) \mathbf{M}_{11}$$

The critical alpha is thus simply

$$\alpha_c = \left[\int dy C(y)^2 \mathcal{Z}_{\text{out}}(y) \right]^{-1} \approx 0.575166 \quad (127)$$

$$\mathbf{F.5} \quad g(z_1, \dots, z_p) = \sum_{j=1}^p \text{sign}(z_p)$$

Following a procedure similar to Section F.3, we define $\omega = (\omega_1, \dots, \omega_p)^{\top}$ and $v_{ij} := (\mathbf{V}^{-1})_{i,j}$. We also introduce the matrix $\mathbf{d}(\mathbf{V}) \in \mathbb{R}^{(p-1) \times (p-1)}$ such that

$$d_{ij}(\mathbf{V}) := \det \begin{pmatrix} v_{i,j} & v_{i,p} \\ v_{j,p} & v_{p,p} \end{pmatrix}, \quad i, j \in 1, \dots, p, \quad (128)$$

the function

$$E_s(\mathbf{z} \in \mathbb{R}^{p-1}, y, \omega, \mathbf{V}) = \frac{1}{2\sqrt{2}v_{pp}} \left(1 - s \cdot \text{erf} \left(\frac{\sum_{i=1}^{p-1} v_{ip}(z_i - \omega_i) - v_{pp}\omega_p}{\sqrt{v_{pp}}} \right) \right), \quad (129)$$

the Gaussian probability density

$$\rho(\mathbf{z} \in \mathbb{R}^p, \mathbf{V}) := \frac{1}{(2\pi)^{p/2} \sqrt{\det(\mathbf{V})}} e^{-\frac{1}{2} \mathbf{z}^{\top} \mathbf{V}^{-1} \mathbf{z}}, \quad (130)$$

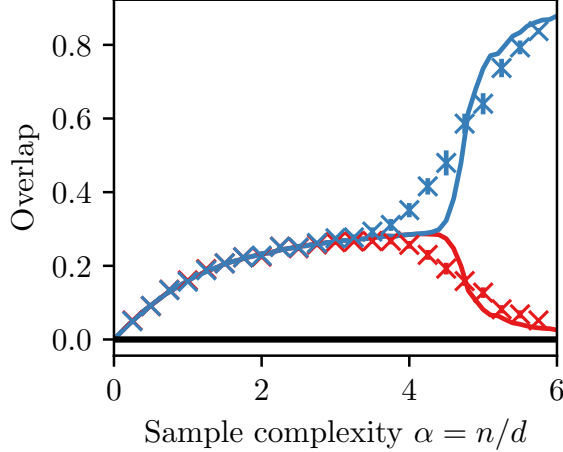


Figure 3: Specialisation as an example of grand staircase with $g = \text{sign}(z_1) + \text{sign}(z_2) + \text{sign}(z_3)$. The direction spanned by $z_1 + z_2 + z_3$ is first learned for any $\alpha > 0$. The remaining ones are only learned at the *specialisation* transition occurring at $\alpha \approx 4.3$. We take care of the symmetries as indicated in S.I. G. Crosses denote AMP runs with $d = 100$ averaged over 72 seeds. The overlap is shown as a function of the sample complexity. Because of the symmetry the elements of M can take one of two values: one on the diagonal and one outside of it. We display $(M_{11} + M_{22} + M_{33})/3$ in blue and $(M_{12} + M_{13} + M_{23})/3$ in red.

and finally

$$I_s(\mathbf{z} \in \mathbb{R}^{p-1}, y, \boldsymbol{\omega}, \mathbf{V}) = v_{pp}^{(p-1)/2} E_s(\mathbf{z}, y, \boldsymbol{\omega}, \mathbf{V}) \rho \left(\begin{pmatrix} z_1 - \omega_1 \\ \dots \\ z_{p-1} - \omega_{p-1} \end{pmatrix}, v_{pp} \mathbf{d}(\mathbf{V})^{-1} \right).$$

Then, defining $\mathbb{R}_{+1} = [0, +\infty)$ and $\mathbb{R}_{-1} = (-\infty, 0]$, we have that

$$\mathcal{Z}_{\text{out}} = \sum_{\substack{s_1, \dots, s_{p-1} = \pm 1 \\ |\sum_{i=1}^{p-1} s_i - y| = 1}} \int_{\mathbb{R}_{s_1}} dz_1 \dots \int_{\mathbb{R}_{s_{p-1}}} dz_{p-1} I_{y - \sum_{i=1}^{p-1} s_i}(\mathbf{z}, y, \boldsymbol{\omega}, \mathbf{V}), \quad (131)$$

and the k^{th} component of $\mathbf{g}_{\text{out}}(y, \boldsymbol{\omega}, \mathbf{V})$ is

$$(\mathbf{g}_{\text{out}}(y, \boldsymbol{\omega}, \mathbf{V}))_k = \frac{1}{\mathcal{Z}_{\text{out}}} \sum_{\substack{s_1, \dots, s_{p-1} = \pm 1 \\ |\sum_{i \neq k} s_i - y| = 1}} \left(y - \sum_{i \neq k} s_i \right) \int_{\mathbb{R}_{s_1}} dz_1 \dots \int_{\mathbb{R}_{s_p}} dz_p \rho(\mathbf{z} - \boldsymbol{\omega}, \mathbf{V}) \delta(z_k)$$

G Further numerical observations

Here we give more details about the numerical implementation of State Evolution and AMP. Both approaches require to compute \mathbf{g}_{out} . All the examples we implemented are detailed in S.I sec. F.

The integrals are doing with the quadrature package in Scipy. In order to avoid instabilities we regularize the interval of integration by replacing ∞ with Λ . We typically choose $\Lambda \approx 10$. Similarly, we add $\epsilon \approx 10^{-4}$ to the diagonal of V . In State Evolution we need to integrate over functions of \mathbf{g}_{out} . We do these integrals using a simple Monte Carlo approach. For Figure 1 we used a total 72000 samples, for Figure 3 7200. Computing such integrals is the numerical bottleneck. In order to make this part faster we parallelised the MCMC: for each iteration of State Evolution we make every worker in our pool estimate the integral, and then average the estimation and then average among workers. In the cases in which $\mathbf{M} = 0$ is a fixed point, we initialize \mathbf{M} with the empirical overlap of AMP at the beginning of the iteration.

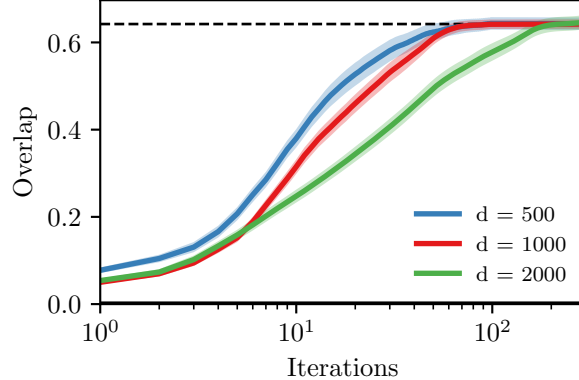


Figure 4: Trajectories of 16 AMP runs with random initialisation at $\alpha = 4$ for $g(z_1, z_2) = \text{sign}(z_1 z_2)$. The shaded areas represent the error on the mean. We can see that as the dimension increases the algorithm gets increasingly slower

In both the AMP and State Evolution implementation we used some damping: the overlap \mathbf{M} or the $\hat{\mathbf{W}}$ at the new iterations are averaged with the current value, with a weight δ for the new one, where typically $0.6 < \delta < 0.9$. We display the evolution of the overlaps in a typical run of AMP for the model $z_1^2 + \text{sign}(z_1 z_2 z_3)$ in Figure 2. We already displayed the values of the overlap and generalisation error at convergence in Figure 1. We can see how AMP has a saddle-to-saddle dynamic, where the algorithm alternates plateaus for $\mathcal{O}(\log d)$ iterations to fast drops in generalisation error, which are associated with new directions being learned. We probe experimentally the dependence on size in Figure 4. All the error bars present represent the error on the mean. We used the local computing cluster for our experiments. In particular we needed around 40 CPUs with 72 cores each and approximately 3 Gb per core.

As stated in the main text, models non-trivial subspaces are associated with symmetries. This also implies that the associated overlaps are have the same invariances. In order to make the plots readable we remove all such symmetries by hand. For this reason we take the absolute value of the overlap if the model is even, and we impose a specific inequality in the overlap if there is invariance under permutation. As a general idea we want to always have the "best" possible overlap. Meaning we want \mathbf{M} to be as diagonal as possible. We list what this mean for the examples in the figures:

- $\text{sign}(z_1 z_2)$: Because of invariance under exchange of z_1 and z_2 we always have $\mathbf{M}_{11} = \mathbf{M}_{22}$. Here AMP can reach 2 equivalent configurations: either the diagonal or the anti-diagonal is zero. We choose the configuration where the anti-diagonal is zero.
- $z_1^2 + \text{sign}(z_1 z_2 z_3)$: This model will first learn just z_1 . We fix $\mathbf{M}_{11} > 0$. For the rest of the components we are reduced to the case above.
- $\text{sign}(z_1) + \text{sign}(z_2) + \text{sign}(z_3)$: Because of the invariance under permutation each row of \mathbf{M} will have either the same element in all the entries (in which case we don't need to do anything) or two are the same and one is bigger. We permute the matrix such that the largest entry is on the diagonal.

The code to run AMP and State Evolution on the examples in the is available on GitHub
<https://github.com/SPOC-group/FundamentalLimitsMultiIndex>